Arabian Journal of Geosciences (2024) 17:109
https://doi.org/10.1007/s12517-024-11896-6

ORIGINAL PAPER

Simultaneous removal of fluoride and arsenic from drinking groundwater using limestones from Bajío Guanajuatense, Mexico

Fátima Juárez-Aparicio[1] · José Iván Morales-Arredondo[2] · María Aurora Armienta Hernández[2]

Received: 23 May 2023 / Accepted: 25 January 2024 / Published online: 29 February 2024

Abstract

Numerous groundwater wells in Mexico exceed the maximum allowable fluoride (F^-) and arsenic (As) drinking water concentration requirements, posing an environmental and health risk to the population that relies solely on these wells for drinking water sources. Since encouraging results have been obtained utilizing native limestones to remove some toxic elements from contaminated water, the ability of the limestone rock outcrop to the south of the Sierra de Guanajuato in Mexico to remove As and F^- from groundwater was assessed. A sampling campaign was conducted in the study area, focusing on wells exhibiting elevated concentrations of arsenic (As) and fluoride (F^-) in compliance with international standards. This water was employed in the treatment experiment involving limestone rocks. The rock sampling process involved a reconnaissance campaign covering the study area and outcrop points of limestone rocks. Representative limestone samples were collected and subsequently subjected to mineralogical and geochemical characterization. Using rock samples, synthetic water, and groundwater from contaminated wells in the region, batch experiments were conducted to evaluate the As and F^- removal capacity of limestone. The batch testing consisted of water–rock interactions at various times with different samples of limestone rocks, grain sizes, and water containing distinct concentrations of both elements, artificial and groundwater extracted close to the limestones outcrop. The results indicate that the rock with the highest calcium carbonate ($CaCO_3$) content and the smallest grain size (< 0.05 mm) removes the highest concentrations of both As and F^-, with As removal being superior. The removal mechanisms were studied using scanning electron microscopy with energy-dispersive spectroscopy (SEM–EDS) images, saturation index calculations, and Eh–pH diagrams,. Fluoride precipitation was favored when the pH of the solution was slightly acidic, whereas sorption was favored when the pH was higher. The results obtained are encouraging for the removal of high levels of As, and to a lesser extent for F^-; consequently, the use of regional limestone rocks could be a viable option for improving the water quality ingested by rural inhabitants in the study area. Calcium carbonate ($CaCO_3$) concentration can be used to identify limestone rocks with the potential to effectively remove As and F^- in other locations.

Keywords Limestone · Arsenic · Fluoride · Removal capacity · Groundwater pollution

Introduction

The presence of arsenic (As) and fluoride (F^-) in drinking water is of great global significance, as highlighted by a number of studies (Reardon and Wang 2000; Xiaodong et al. 2020; 2021). According to the World Health Organization (WHO 2018), over 150 million individuals across the globe are exposed to levels of As and F^- in their drinking water that are considered hazardous; prolonged exposure to these chemicals has been associated with various health effects; for instance, the ingestion of F^- has been linked to dental and skeletal fluorosis, renal damage, and cognitive deficits (Gonsebatt and Del Razo 2018; Peiyue L et al. 2002; Miaojun et al. 2021). Similarly, the consumption of As has

Responsible Editor: Amjad Kallel

✉ José Iván Morales-Arredondo
ivanma@igeofisica.unam.mx

[1] Earth Sciences Postgraduate Program, University National Autonomous of Mexico, University City No. 3000, Col. Copilco University, Coyoacán Delegation, 04510 Mexico, CDMX, Mexico

[2] Natural Resources Department, Institute of Geophysics, National Autonomous University of Mexico, Ciudad Universitaria No. 3000, Col. Copilco Universidad, Coyoacán Delegation, 04360 Mexico, CDMX, Mexico

been associated with hyperkeratosis and even cancer (Gonsebatt and Del Razo 2018; Peiyue L et al. 2002; Miaojun et al. 2021). As a result of both natural and anthropogenic processes, it is possible for these elements to be present in groundwater at elevated levels (Bundschuh et al. 2021; Edmunds & Smedley 2013).

Groundwater serves as the primary drinking water source in Mexico, particularly in densely populated urban areas and remote rural communities; extensive detection of groundwater contamination caused by various elements has been documented across the entire country (Armienta et al. 1997; Armienta and Segovia 2008; Jiménez et al. 2018a, b; Rodríguez et al. 2001, 2015). The implementation of water treatment plants is a commonly employed strategy to mitigate the ingestion of contaminated water. However, it is generally more advantageous to explore alternative sources of drinking water in order to obtain supplies of good quality, primarily due to lower costs and ease of implementation (Webb and Davis 2016). Nevertheless, in certain remote rural communities in Mexico, this approach is not feasible due to water scarcity that significantly impacts a substantial portion of the country's territory and necessitates comprehensive management solutions.

The utilization of native limestone to remove potentially hazardous substances, such as As and F^-, represents a sustainable and economically viable approach that can be employed to guarantee individuals with limited financial resources to obtain safe and good-quality drinking water (Litter et al. 2012; Labastida et al. 2019). The efficacy of limestone in removing dissolved arsenic from water is widely recognized in the context of batch treatment, wherein carbonates are precipitated as the pH increases; during this process, hydrogen carbonate ions are converted into carbonate ions, leading to the precipitation of calcium carbonate; it is important to note that the efficiency of this removal process is dependent on the pH level, and the removal efficiency is found to be higher for As(V) compared to As(III). The above process results in the formation of a calcium arsenate precipitate characterized by its restricted solubility. This precipitate, referred to as hydrated calcium arsenate or arsenate apatite, is chemically represented as $Ca_5(AsO_4)_3OH$ (Webb and Davis 2016). Furthermore, the removal of F^- can be done via sorption/desorption mechanisms that involve the formation of external sphere complexes and fluorite precipitation (Labastida et al. 2017). The dissolution of calcite in wastewater leads to the increase of calcium concentration followed by precipitation of fluorite enabling the removal of F^- ions during the process of fluorite precipitation (Reardon and Wang 2000). The removal of F^- from water is influenced by various physicochemical properties, including the concentration of calcium carbonate (Labastida et al. 2017). Reardon and Wang (2000) identified two distinct methodologies for the removal of fluoride from wastewater. There are two primary methods for removing fluoride from a solution: chemical precipitation and sorption techniques, in which fluoride is removed by sorption or ion exchange reactions on a substrate. One of the challenges associated with the removal of As is that observed by Sø et al. (2008); their findings indicate that calcite exhibits little efficacy in removing As, hence suggesting a minimal impact on the mobility of this element. Nevertheless, there are differences in the sorption mechanisms of various arsenic species; for instance, when considering the starting arsenic concentrations evaluated in the experiment, it is shown that little to no sorption of arsenite onto calcite occurs within a 24-h timeframe (0.67 μM). In contrast, it is observed that arsenate exhibits a high affinity for calcite, leading to rapid and efficient sorption; the desorption of arsenate from calcite is also found to be swift and complete within a few hours; this behavior can be attributed to the fact that arsenate does not become integrated into the calcite structure. Furthermore, the extent of arsenate sorption is influenced by the hydrochemical properties of the solution, with higher alkalinity resulting in reduced sorption due to increased competition for sorption sites; the retention of As(V) takes place within a pH range of 7–9 due to the influential role of sorption in controlling the mobility of arsenic, as well as the significance of the Point of Zero Charge; the specific dominant mineral present in each rock being evaluated also affects this process (Romero et al. 2004). Additionally, limestone rocks have been observed to effectively decrease the concentration of As in contaminated water, with desorption levels remaining relatively low (Micete 2005). According to Labastida (2014), the inclusion of limestones in interaction with fluoride content leads to a reduction in the hydraulic permeability of the column system, accompanied by the addition of F^-; there is a scarcity of research investigating groundwater samples with naturally occurring concentrations (Manzo 2019). It is interesting that a significant portion of these investigations have employed artificially prepared water; while others have focused on wastewater samples, several experiments conducted using synthetic water have shown promising outcomes in the removal of As and F^-; however, it remains uncertain whether similar results can be achieved with groundwater due to potential constraints imposed by hydrogeochemical processes, such as ionic competition or reaction kinetics (Sosa 2019).

In accordance with the favorable outcomes observed in previous studies (Labastida 2014; Labastida et al. 2017; Micete 2005) regarding the removal of As and F^- through experiments utilizing Mesozoic limestone (specifically the Soyatal Formation) from various geographical areas, an assessment was conducted to evaluate the effectiveness of limestone samples obtained from the southeastern region of the Sierra de Guanajuato in reducing elevated levels of As and F^- in the local groundwater. Limited research has been

conducted on the filtration capabilities of this particular geological substance in relation to groundwater (Manzo 2019). This scarcity of studies can be attributed primarily to the presence of additional ions in the water, which can impact the removal process (Sdiri et al. 2012; Sdiri & Higashi 2013; Sosa et al. 2020). Nevertheless, calcite exhibits potential as a viable and cost-effective treatment method for water contaminated with arsenic (As) and fluoride (F^-). The main objective of this research was to determine the Mesozoic limestone rock within the chosen study region that exhibited the greatest potential for removing As and F^- ions. Additionally, the study aimed to assess the mineralogical and physicochemical factors that influence this removal process, as well as the geochemical retention mechanisms responsible for the observed removal. To achieve these objectives, batch experiments were conducted using both artificial water and groundwater samples obtained from contaminated wells within the study area. This study examines two rural communities with low-income backgrounds that are facing challenges related to drinking water contamination. The contamination is primarily caused by naturally occurring high levels of arsenic (As) and fluoride (F^-) in groundwater, which exceed the limits set by the Mexican drinking water standard, NOM-127 [2000]. These communities are situated in the western Celaya Valley Aquifer, located in Guanajuato, Central Mexico (Morales et al. 2016a and Morales et al. 2016b). The only possible supply of potable water for the entire population is derived from groundwater. The socioeconomic disadvantage experienced by these populations poses additional challenges in addressing the issue.

Background

Santa Cruz de Juventino Rosas and Villagrán are situated in the Bajo Guanajuatense region, which is located in the central-southern part of the Mexican state of Guanajuato (Valverde and Castillo 2002). These two towns are located within the UTM coordinates 14Q287703.92–14Q298406.7 and E 2268 346.23–E 2286895.29 (shown in decimal degrees as longitude − 101.036° and − 100.935°, and latitude 20.502°–20.671°) (Fig. 1). The climate in the region can be classified as semi-arid, characterized by average annual precipitation of 628 mm. The temperature in this area varies between 6 and 31° C, as reported by INEGI in 2020.

General geology

The research region consists of Mesozoic marine sedimentary rocks, specifically shales, sandstones, and limestones that were deposited in a marine environment (Kss). Some of these rocks have undergone a minor degree of metamorphism, resulting in the formation of phyllites, slates, and marble, which belong to the greenschist facies (del Río-Varela et al. 2020). Within the northern region of the designated study area, the Sierra de Guanajuato functions as a geographical boundary, predominantly characterized by the presence of rhyolite-ignimbrite rocks, specifically identified as Tom and Tvr (for instance, Chichindaro rhyolite). Additionally, basaltic and andesitic rocks, identified as Tmb and Tmo (such as La Ordeña andesite), are also found in this area (Río-Varela et al. 2020). The southern portion of the area is mostly characterized by monogenetic volcanoes that are part of the Michoacán-Guanajuato Field. These volcanoes are predominantly comprised of basaltic materials and are situated within the broader Trans-Mexican Volcanic Belt. The ignimbrites, identified as Tom, are found in a significant proportion of the research region. The basin plain contains sediments that have originated from lacustrine-alluvial processes (Qal) (Morales-Arredondo et al. 2018a).

Mineralogy

Limestones consist of calcium carbonate ($CaCO_3$), silicon dioxide (SiO_2), and small amounts of phyllosilicates, likely of the smectite or chlorite types, and muscovite. The classification of rocks as either limestone (RC-1701) or metamorphic limestone (DD1705 and DD1706) is determined by the percentage of $CaCO_3$ present. Metamorphic limestone, in comparison to limestone, contains minerals such as quartz and clays in smaller quantities (Morales-Arredondo et al. 2022). The rocks in question exhibit mineralogical evidence and textural characteristics, such as a microcrystalline texture, iron (Fe) oxyhydroxide laminations, a high SO_4 content, and calcite veins of hydrothermal and tectonic origin. Based on these observations, it is likely that these specimens originate from the Esperanza Formation, as suggested by previous studies (Baez 2012; Echegoyén et al. 1970; Mengelle-López et al. 2013), rather than the Soyatal Formation. The representative volcanic rocks found in the study area consist of various types. These include tholeiitic basalt, which contains pyroxene microphenocrysts that have been replaced by opaque minerals. Another type is vitreous tuff, characterized by lithic fragments composed of a vitreous matrix within a Fe-oxyhydroxide (Fe-ox M) matrix. Lepidolitic vitreous tuff is also present, with lithic fragments of perlitic glass dispersed throughout a vitreous matrix. Altered vitreous tuff is another rock type, characterized by a matrix composed of a vitreous paste containing oxides, Fe-oxyhydroxides (Fe-ox), feldspars (Felds), and quartz (Qz). Additionally, ignimbrite can be found in the study area, with a matrix formed

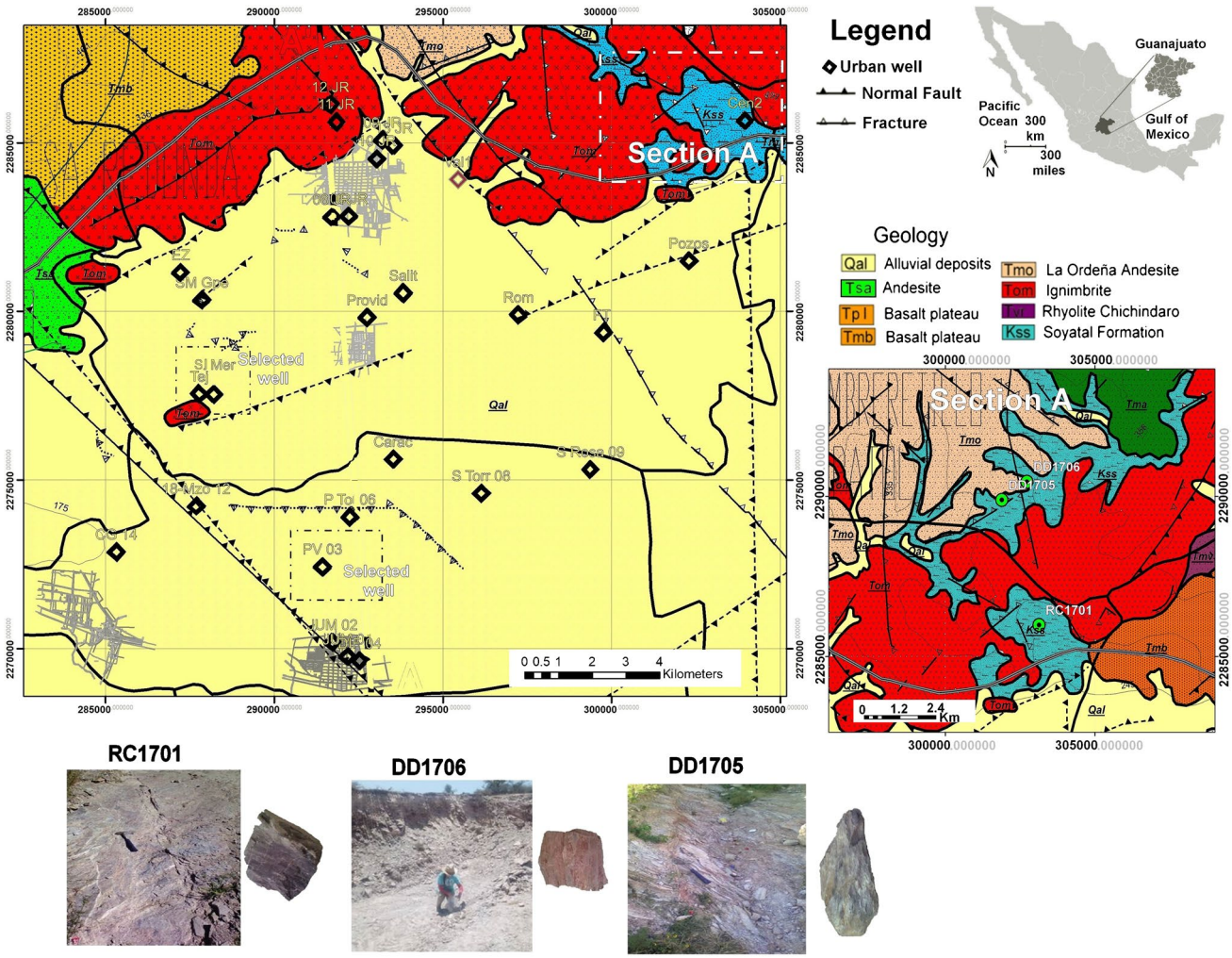

Fig. 1 Location of the study area, geological map, and location of the wells and sampled rocks. Squared areas mark the wells used in this study. Zoom view with the location and photographs of the sampled limestone rocks, RC1701, DD1706, DD1705. The sampled material consists of Mesozoic marine rocks (shales, sandstones, and limestones deposited under marine conditions) (Kss), classified as limestone (RC1701) or metamorphic limestone (DD1705 and DD1706)

by an alignment of vitreous fragments. Some veins can be observed obliquely cutting across fiammes. Lastly, ignimbrite tuff is present, characterized by a vitreous matrix containing quartz and clay mineral veins that replace feldspars. Biotites in this rock type are moderately replaced by chlorite (Morales-Arredondo et al. 2018c). The constituents of sedimentary deposits include conglomerates, clays, sandstones, and gravel.

Groundwater

The hydrogeological characteristics of the JR region are notably influenced by its geological framework, including volcanic formations exhibiting diverse acidic and basic compositions, as well as a sedimentary basin containing lacustrine-alluvial deposits commonly referred to as Qal (Morales-Arredondo et al. 2018a). In the geographical area of Juventino Rosas Villagrán, certain wells that serve as sources of potable water for the various communities have been determined to have poor quality in terms of their As and F^- content, as per the guidelines outlined in NOM-127-SSA-2001. The issue of compromised water quality has been identified in Juventino Rosas since 2010, and in Villagrán since 2017 (although reports suggest that the problem precedes these years for both municipalities) (Fig. 2a, b). This prevailing circumstance poses an environmental concern within the region, given that groundwater represents the sole accessible source of water for the local population (Fig. 2c, d; with a population of 82,340 inhabitants in Juventino Rosas and 65,791 inhabitants in Villagrán). In relation to water treatment, it is notable that both municipalities own

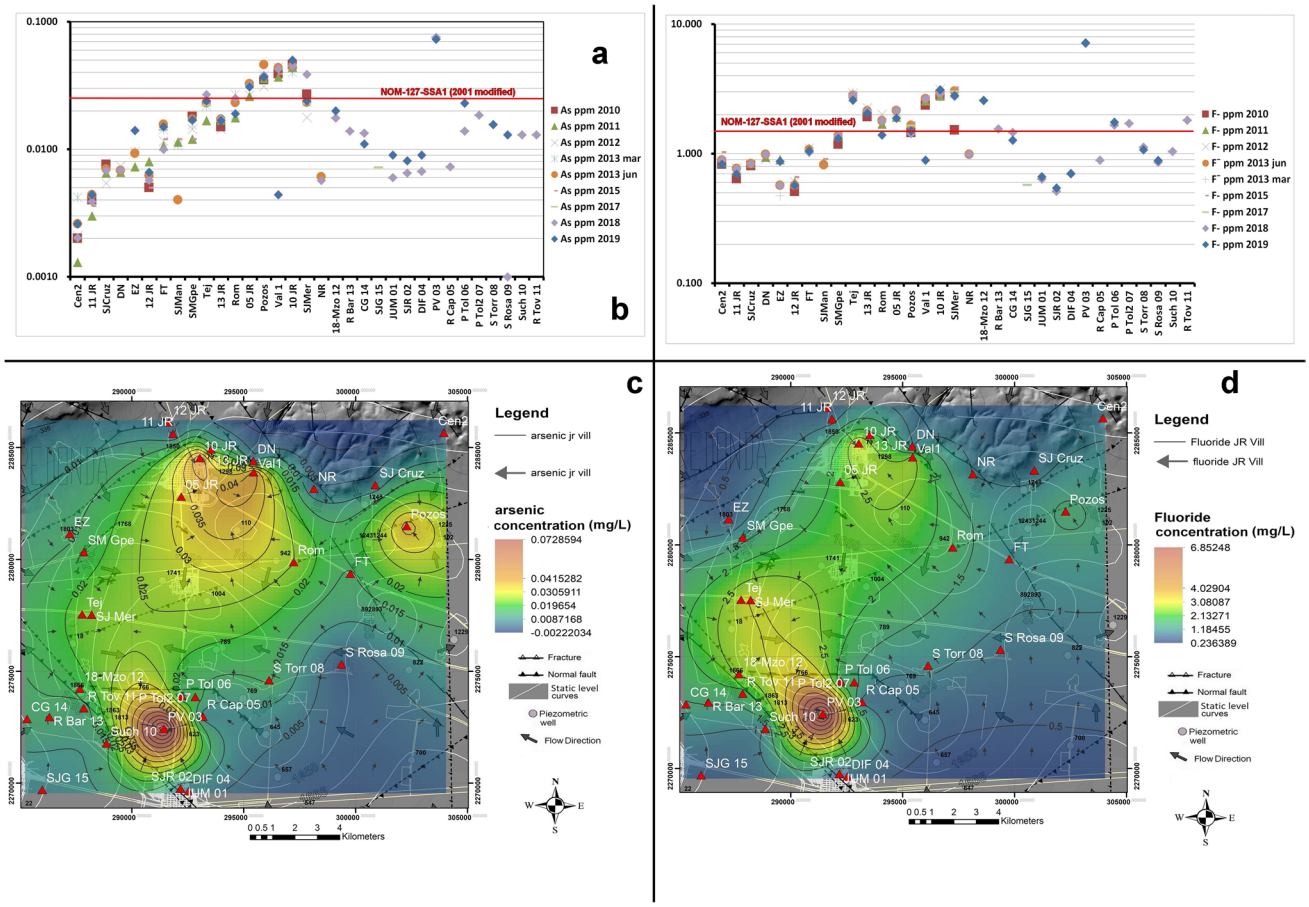

Fig. 2 The temporal (**a**, **b**) and spatial (**c**, **d**) concentrations of As and F^- in two municipalities located in "El Bajío Guanajuatense," Guanajuato State, Mexico

a limited number of wastewater treatment plants, with Santa Cruz de Juventino Rosas having a sole drinking water treatment facility that employs a softening technique (CONAGUA (Comisión Nacional del Agua), 2015).

Materials and methods

Sampling methodology

Rock sampling

The collected samples consist of Mesozoic marine rocks, specifically shales, sandstones, and limestones. These rocks are further categorized as limestone (RC1701) and metamorphic limestone (DD1705 and DD1706). One of the factors influencing the selection of these rocks was ascertain if whether all limestone rocks have the same removal capacity or only some with certain characteristics. The outcrop sites of three Mesozoic representative limestone rocks (DD1705, DD1706, and RC1701) is shown in Fig. 1.

Groundwater sampling

A sampling campaign was carried out in 2019, with an environmental focus on the drinking water of two wells located in two rural communities within the research area. The wells included in this study were chosen from a total of 32 sites that supply water to a population of approximately 148,000 individuals (Fig. 2c, d). The selection criteria mostly focused on the levels of As and F^- present in the water, which exceeded the established drinking water requirements in Mexico. These wells were primarily selected for practical purposes in order to facilitate the performance of the experiments. One of these wells contains the highest concentration of As and F^- among the 32 sampled wells, while another also contains a high concentration of both elements. There had been previous physicochemical analyses of the wells (Morales et al. 2016a and Morales et al. 2016b, Morales-Arredondo et al. 2018a, Morales-Arredondo et al. 2022). The water sample procedure adhered to the guidelines outlined in NOM-014-SSA1-1993 and APHA (2005) regulations. The accuracy of the results was confirmed through the utilization of an ionic balance.

Material pre-treatment of sampled rocks

The rocks were crushed and sieved, and the sample particle sizes of 0.5–1.41 mm and < 0.05 mm. This selection was determined by previous studies conducted by Micete in 2005, which showed favorable outcomes in the removal of As and F^- from batch systems. The inclusion of the data for rock sample DD1706 as supplemental material (SMF 1 to 6, SMT 1 to 3) is justified by the observed similarities between rock sample DD1705 and DD1706.

Mineralogical evaluation

In order to analyze the limestone samples collected from the study area, X-ray diffraction (XRD) was conducted on rocks that had been sieved to a mesh size of less than 75 m. This analysis was carried out using an EMPYREAN diffractometer, which was equipped with a nickel (Ni) filter, a fine focus copper tube, and a PIXcel3D detector. The XRD analysis was performed at the Laboratorio de Difracción de Rayos X of the Institute of Geology, UNAM.

X-ray fluorescence

The major elements in the samples (which were sieved at a size smaller than 0.5 mm) were analyzed using X-ray fluorescence (XRF) at the Laboratorio Nacional de Geoquímica y Mineralogía of the Institute of Geology, UNAM. The analyses were conducted using a RIGAKU ZSX Primus II spectrometer. In the X-ray fluorescence (XRF) investigations, the powdered specimen was amalgamated and fused with a mixture consisting of 50% $Li_2B_4O_7$ and 50% $LiBO_2$. The amount of volatile components, referred to as the loss on ignition (LOI), was ascertained by subjecting the sample to a temperature of 950 °C. The elemental composition was reported in the form of oxide compounds.

Determination of specific surface

The specific surface area of each limestone sample was determined using the sorption technique and the Brunauer–Emmett–Teller (BET) isotherm. The pore size distribution of the RC1701 rock was analyzed for two different grain sizes, specifically 0.5–01.41 mm and less than 0.05 mm. Additionally, the pore size distribution was calculated for the DD1706 and DD1705 rocks, both of which had a grain size smaller than 0.05 mm. The specific area of interest was determined using the BET method, employing a Quantachrome brand Autosorb-1 instrument. The rocks included in the batch trials were produced, as stated by Micete (2005).

Determination of As concentration in limestone

The concentration of total As was quantified in the acid-digested rocks using the CEM MARS Xpress microwave oven, both prior to and subsequent to the batch testing. The laboratory's available analytical techniques did not allow for quantifying the fluoride ion concentration in the rock samples. The process of quality assurance was carried out by the digestion and analysis of the reference standard material NIST 2709. The concentration of arsenic was determined by hydride generation, utilizing a Perkin Elmer AAnalyst 200 atomic absorption spectrometer and FIAS 100 system. To ensure the accuracy, quality, and reliability of the analyses for both element, certified solutions that are traceable to the National Institute of Standards and Technology (NIST) were employed. The standard sample exhibited a 40% recovery for As due to the distinct matrix (NIST 2709, not composed of limestone) and the fact that the concentrations obtained before digestion with a mixture of 3HCl and HNO_3, which reflected pseudo-total concentrations rather than actual total concentrations.

Well groundwater characterization

The physicochemical parameters (pH, electrical conductivity (EC), temperature, and oxidation–reduction potential (ORP)) were monitored in situ using a field multi-parameter device (HANNA HI9829) that was calibrated previously. The principal ions present in the samples were subjected to chemical tests at the Analytical Chemistry Laboratory of the Institute of Geophysics, UNAM, Mexico. The procedures employed for these analyses were in accordance with the APHA-AWWA guidelines from 2005. The determination of hydrogen carbonate was conducted using volumetry via HCl titration with a volumetric concentration (VC) of 6%. Similarly, the determination of Ca^{2+} and Mg^{2+} ions was carried out by volumetry using titration with EDTA, with a VC of 1%. The measurement of Cl^- ions was quantified by potentiometry using selective electrodes, with a VC of 1%, following the 4500-Cl^- method as outlined in the APHA-AWWA 2005 guidelines. The measurement of Na^+ and K^+ ions was performed using atomic emission spectrophotometry, with respective VCs of 1.1% and 0.7%, following the 3500-Na^+ and K^+ methods as specified in the APHA-AWWA 2005 guidelines. Lastly, the determination of SO_4^{2-} ions was carried out by turbidimetry, with a VC of 1%, following the method 4500-SO_4^{2-}. The ionic balance of the geothermal water samples was found to be less than

10%. Specifically, only one sample had ionic balance values beyond 5%, while the remaining wells demonstrated values below this threshold. The contents of As and F^- were determined at the Analytical Chemistry Laboratory of the Geophysics Institute. Arsenic concentrations were measured using a Perkin Elmer model AAnalyst 200 flame atomic absorption spectrometer, coupled with a Perkin Elmer FIAS 100 hydride generator, by the NMX-AA-051-SCFI-2016 standard. The detection limit for As using the equipment was 0.001 mg/L. The concentration of F^- was measured using potentiometry using a selective ORION electrode, namely the Thermo Scientific Orion 5 Star. The detection limit for F^- using the same equipment was determined to be 0.005 mg/L. Quality control included checking the accuracy with certified "High Purity Standards" solutions (NIST traceable), using blanks, determining the average of three replicates for each sample, and analyzing standards for every 5 samples.

Synthetic solutions

Synthetic solutions simulating As and F^- concentrations in samples from wells SJMer and PV03 (Fig. 1) were prepared using sodium fluoride (NaF) and sodium arsenate dibasic heptahydrate ($Na_2HAsO_4{\cdot}7H_2O$) salts of analytical quality. The pH and EC values of each of the prepared solutions were measured.

Hydrogeochemical modeling of groundwater samples

The software Geochemist's Workbench (GWB Student 12.0) was utilized to analyze the data derived from the well water samples. The GWB's Act2 program was employed to generate Piper and Eh–pH diagrams to determine the species of As present in the well waters. Furthermore, the GSS spreadsheet application was employed to calculate the ionic strength in conjunction with GWB. The GBW program uses a range of geochemical databases to do geochemical analysis and modeling. Among these databases, the file named "thermo.tdat" is often utilized. The database includes a comprehensive range of thermodynamic data many chemical species. Accurate thermodynamic calculations are essential for various applications, including the prediction of mineral solubility, determination of chemical element speciation in solution, and geochemical modeling. The provided information is valuable due to the presence of thermalism in a specific area, which is distinguished by the occurrence of mildly alkaline water, a neutral pH, and oxic to suboxic Eh values. The inclusion of a vast array of chemical reactions and thermodynamic equilibria in this database facilitated the acquisition of comprehensive findings about geochemical processes. Moreover, the geological environment of the region is characterized by its complexity.

Kinetic studies and removal experiments

Before beginning the removal tests, an evaluation was conducted to determine the levels of As and F^- generated by water–rock interaction for each of the rock samples. These assessments were carried out under standard conditions of pressure and temperature, with an initial water pH of 4.98 and an electrical conductivity (EC) of 18.2 µS/cm. After the stage of agitation, the samples were centrifuged and filtered using a 0.45-µm filter. After this, an analysis was conducted on the solution to determine the pH, and the electrical conductivity (EC), as well as the concentrations of As and F^- (RC1701 = 7.78, DD1706 = 7.74, and DD1705 = 7.91 for the ultimate pH). Similarly, water removal experiments were performed with synthetic solutions of As and F^- only (under standard conditions of pressure and temperature, the initial pH in synthetic solution was approximately 5.5 $EC_{PV} = 40$µS/cm and $EC_{SJMer} = 17.3$ µS/cm); the tests were carried out in duplicate and consisted of three stages: the first evaluation was conducted on each rock with a NaF solution (to obtain similar F^- concentrations measured in both wells); the second was evaluated on each rock using solutions containing arsenate (AsO_4^{3-}) to achieve similar As concentrations measured in both wells. Two solutions were prepared using sodium fluoride (NaF), and two solutions using the reagent sodium arsenate heptahydrate ($Na_2HAsO_4{\cdot}7H_2O$) and deionized water to simulate the concentrations of fluoride (PV = 7.2 mg/L, and SJMer = 2.8 mg/L), and arsenic (PV = 0.073 mg/L, and SJMer = 0.039 mg/L); in each solution, the pH and EC were measured (Table 1).

Then, RC1701, DD1705, and DD1706 rocks with grain size < 0.05mm and 0.5–1.41mm were subjected to orbital shaking at a speed of 170 rpm (in a 1:5 ratio of rock-water), for 1, 5, 24, 48, and 72 h. The aqueous phase was centrifuged and filtrated with 0.45-µm Millipore membranes. The membranes were dried and stored for future analysis. The final measurements included pH, EC, and F^- concentrations (final pH ranged from 7 to 8.5 and EC ranged from 100 to 120 µS/cm for the synthetic solution of NaF; final pH ranged from 7.4 to 8.7 and EC ranged from 50 to 170 µS/cm for the synthetic solution of $Na_2HAsO_4{\cdot}7H_2O$). Histograms of the percentage of removal and pseudo equilibrium diagrams were constructed.

The third stage of the study involved assessing the efficacy of rock removal by utilizing water samples obtained from SJMer and PV03 wells (at standard conditions of

Table 1 Physico-chemical characterization of PV03 and SJMer wells. Arsenite concentration compared to total As present in the wells. (*EC* electrical conductivity, *I.B.* ionic balance), and mineralogy (X-RD) and chemical (X-FR) composition of limestone rocks, (*) = Total percentage o major elements of Kit-1. *D.L.* detection limit

	Well	pH	EC (µS/cm)	T (°C)	Cl^- (mg/L)	SO_4^{2-} (mg/L)	HCO_3^- (mg/L)	CO_3^{2-} (mg/L)	Na^+ (mg/L)	Mg^{2+} (mg/L)	Ca^{2+} (mg/L)	K^+ (mg/L)	As (µg/L)	F^- (mg/L)	I.B. (%)	Eh_{cal} (mV)	As^{3+} (µg/L)	As_{tot} (µg/L)	Ionic Strength (I)
Groundwater results	Praderas de la Venta (PV03)	8.19	862	39.5	30.9	27.1	247.57	25.73	129.8	1.38	4.57	9.99	**73**	**7.2**	2.4	128.7	1.7	7.3	0.0067
	San José de Merino (SJMer)	7.74	491	45.6	10.6	20.0	254.71	9.8	94.5	5.52	10.55	9.92	**39**	**2.8**	4.1	88.8	0.2	39	0.0057
	D.L	–	–	–	0.04	4.0	0.3		1.0	0.8	0.8	0.5	0.001	0.1	–	–	–	–	–
X-RD	Sample	Calcite (%)		Quartz (%)		clay (smectite) (%)			clay (kaolinite) (%)			Micas (muscovite) (%)				Hematite (Fe_2O_3) (%)		total (%)	
	RC1701	66		29		5												100	
	DD1706	38		36		8						16				2		100	
X-RF	Sample	**SiO_2** (%)	**TiO_2** (%)	**Al_2O_3** (%)	**Fe_2O_3t** (%)	**MnO** (%)	**MgO** (%)		**CaO** (%)		**Na_2O** (%)	**K_2O** (%)		**P_2O_5** (%)		**LOI** (%)		**Total** (%)	
	RC1701	16.147	0.094	1.751	0.882	0.05	0.449		44.721		0.044	0.263		0.078		35.48		99.959	
	DD1706	35.392	0.208	4.693	2.515	0.133	0.793		30.192		0.043	0.918		0.158		25		100.045	
	Kit-1 Internal reference material	7.81 (7.79*)	0.091 (0.1*)	1.672 (1.96*)	0.65 (1.13*)	0.015 (0.02*)	0.473 (0.41*)		48.671 (49.31*)		0.168 (0.11*)	0.292 (0.53*)		0.053 (0.05*)		40.06 (35.5*)		99.96 (96.54*)	

pressure and temperature, the initial pH in synthetic solution was ~ 7.74 in SJMer and 8.19 in PV and EC were = 862µS/cm and 491 µS/cm respectively). The methodology included the assessment of multiple physicochemical parameters in order to consider the presence of additional chemical species (Table 1). The experimental procedure involved conducting trials using a rock–water ratio of 1:5, and the mixture was stirred at 170 rpm in orbital shakers for varying amounts of time (1, 5, 24, 48, and 72 h). Each experiment's aqueous phase was centrifuged and filtered using 0.45-µm Millipore brand membranes. The membranes containing the filtered fraction were dried and preserved for analysis at a later time. Finally, the pH, EC, and concentrations of As and F^- were measured (final pH ranged from 8 to 8.5, and EC value ranged from 400 to 550 µS/cm for water well from PV in interaction with all rocks; final pH ranged from 8 to 8.5, and EC value ranged from 420 to 600 µS/cm for water well from SJMer in interaction with all the rocks).

Histograms were developed to represent the % elimination. The estimation of the removal efficiency of the pollutants was conducted using the subsequent equation:

$$\% = \frac{c_0 - c_f}{c_0} 100 \quad (1)$$

where c_0 is the initial concentration and c_f is the final concentration.

Analysis of precipitates

The rock samples exhibiting the greatest degree of removal were subjected to analysis using MEB-EDS.. The analysis was performed using a JEOL electronic microprobe JXA-8900R at the University Petrographic Laboratory. The sample was prepared by placing an adhesive tape on a glass support, adhering to the fine precipitate (< 0.05 mm), and coating it with graphite to create a conductive surface. At the end of the preparation procedure, the sample was subjected to measurement after its placement within an aluminum sample holder.

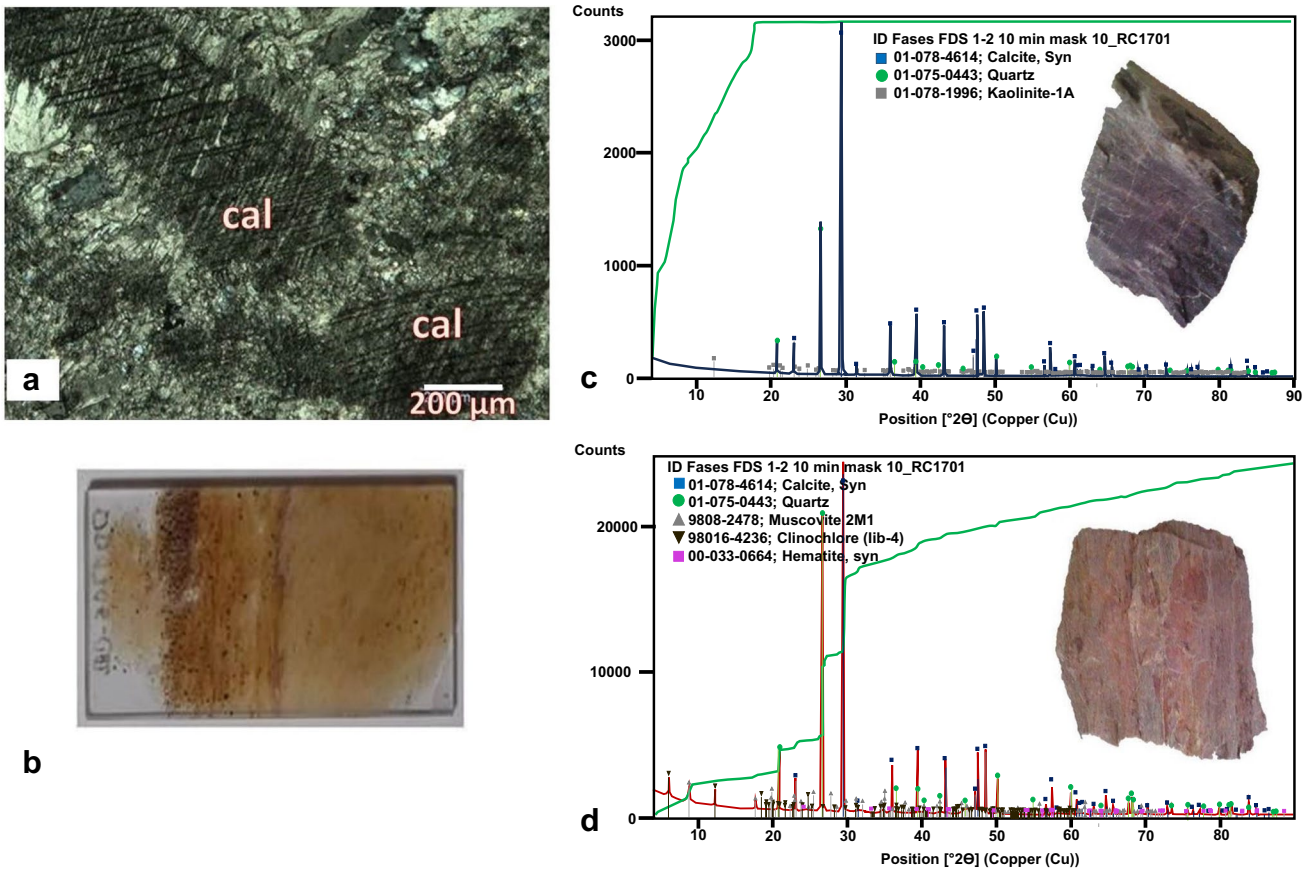

Fig. 3 **a** RC1701 light microscopy image, **b** DD1706 light microscopy image, **c** RC1701 diffractogram, **d** DD1706 diffractogram

Results

Chemical and mineralogical characterization of the rocks

X-ray diffraction and light microscopy

The rock RC1701 exhibits a degree of weathering and crystallized calcite veins, as determined by X-ray diffraction and optical microscopy. In the images taken by light microscopy, the distinctive cruise of calcite and polycrystalline aggregates of calcite and quartz are visible, in addition to quartz detrital grains (Table 1, Fig. 3a, b). The identified phases in sample DD1706 are hematite, as a result of the oxidation process (Table 1 and Fig. 3b, c). In addition, light microscopy images reveal the presence of micas and foliation, indicating a low degree of metamorphism (SMF 1 a and b). The phases identified in rock DD1705 suggest that the rock was altered to a low degree of metamorphism (Table 1 and SMF 1a, b, SMT 1). The presence of iron oxides may have an impact on As removal process since ferric oxide can effectively contribute to the removal of As (Mejía et al. 2009) because As can be sorbed and immobilized when precipitating with Fe oxides (Kefeni et al. 2017; Labastida et al. 2019). In addition, Sparks (2005) found that Fe oxides have a high affinity for sorbing As due to their high specific surface area and high surface charge, which can vary with pH. Some tests carried out with limestone, mixed with precipitation of iron on the surface of the material, have shown that this method is effective for removing both arsenate and arsenite because arsenic is re-sorbed to the iron surface through ionic interactions, especially at low levels and high pH (Webb and Davis 2016). Limestone provides a heterogeneous surface for iron deposition, secondary binding sites, an alkaline surface pH, and buffering capacity enabling the removal of approximately 99% of arsenic.

Although only a small amount of muscovite was found, it can aid in the removal of F^- by substituting OH^- inside its structure with F^- at pH levels greater than 6.5 (Labastida et al. 2017; Singh et al. 2011). In addition, Zhuang and Yu (2002) reported that natural clay minerals are not effective in removing anions, unless they are coated with metal oxides or hydroxides, especially Fe. This is due to the fact that the electrochemical characteristics of clay mineral colloids are frequently influenced in natural environments by metal-oxides (such as Al and Fe) and organic matter, primarily in kaolinite, montmorillonite, illite, and even zeolites (Mejía et al. 2009), since the coatings can increase the specific surface area. This is owing to an increase in positive charges and a decrease in negative charges on the clay surfaces, a shift in the zero point of charge to a higher pH, and the enhancement of fluoride sorption due to the presence of more OH^- and OH_2 on the oxide surfaces compared to the clay surfaces. The precence of micas, clays, and Fe oxides in rocks DD1706 and DD1705 enables these reactions to take place (Table 1, SMT 1).

X-ray fluorescence

The quantitative chemical analysis by XRF confirms the presence of a high amount of calcium (Ca) and silicon (Si) in the rock samples. According to the stoichiometric relationship between $CaCO_3$ and calcium oxide (CaO), the percentage of $CaCO_3$ was determined (Table 1). The RC1701 rock contains the highest concentration of $CaCO_3$, whereas the DD1706 rock contains the least. It was expected that the rock with the highest $CaCO_3$ content would have the greatest removal capacity, and rocks with lower levels of calcite would exhibit beneficial results for the removal of As and F^- due to the presence of other minerals such as hematite and muscovite.

Specific area of the rocks

Based on the BET isotherms, it can be shown that sample DD1706 (and DD1705) had the greatest specific surface area for grain sizes < 0.05 mm. The mineralogy of both rocks shows the presence of clays and Fe oxides (mainly in DD1706). The presence of Fe oxides and the highest specific surface area increase the likelihood of achieving successful As removal. This is due to the fact that a bigger specific surface area suggests a greater capacity for interaction or sorption between the rock and the contaminants, as has been observed in previous research using rocks with high clays and Fe oxides content (Reardon and Wang 2000; Webb and Davis 2016).

Total arsenic concentration in rocks

Prior to the water filtration tests, As concentration was determined in all rocks. The total concentrations of As in the rocks ranged from 1.29 to 5.58 µg/g (with RC1701 containing the highest levels) (Table 2). In addition, water dissolution tests were performed for each rock to assess the concentrations of As and F^- released into the water (agitation time for 72 h, with both grain sizes and a 1:5 rock:water ratio) (Table 2).

The results revealed that the three types of limestones contributed both F^- and As to the water. The sample releasing the most amount of As corresponded to which also had the lowest total As concentration (RC1701). The rocks that released a greater concentration of As and F^- are characterized by a low degree of metamorphism and include more

Table 2 Specific surface and pore size distribution, total As concentration in the rocks, and concentrations of As and F^- released by each rock at 72 h agitation. Total As concentration in rocks (mg/kg) before batch experiments. The identification (ID) 1F, 2F, 3F, and 8F, 9F, and 12F represents the experimental number, total As concentration in rocks (mg/kg) after batch experiments with groundwater samples. Initial rock sample weight = 20 g, water sample volume = 0.1 L, and concentration of As (mg/L) for each sample, removal percentage of As and F^- with synthetic water and well water corresponding to the grain size, and specific surface area of rock samples

Specific area and pore size distribution of rocks				Total As concentration		As and F^- contribution of each rock after batch tests				Total concentrations of As in rocks before batch experiments			Removal percentage of As and F^- with synthetic water and well water corresponding to the grain size, and specific surface of rock samples				Total initial and final As concentrations in groundwater samples, before and after the batch tests		
Rock samples	Grain size (mm)	Specific area (m^2/g)	Pore size distribution (Å)	Total As (mg/L)	Total As (µg/g)	F^- (mg/L)	As (mg/L)	Initial pH (distilled water)	Final pH	Initial EC (µS/cm) (distilled water)	Final C.E. (µS/cm)	ID	Total As (mg/L)	Total As (mg/kg)	Grain size (mm)	Specific Surface (m^2/g)	Maximum removal of F^- (%) synthetic solution	Maximum removal of As (%) synthetic solution	Maximum removal of As (%) well water	Well	As (mg/L) initial	As $(mg/L)_{final}$
RC1701	0.5–1.41	0.73	261.4	0.112	5.58	**0.177**	**0.001**	4.98	7.78	18.2	165.85	1F	0.1118	5.58	< 0.05	2.34	47.86	95.39	30.28	56.67	SJMer	**0.039**	0.011
												2F	0.0315	1.58									
RC1701 (a)	< 0.05	2.34	306																				
DD1706	< 0.05	4.99	233	0.0315	1.58	**0.403**	**0.003**	4.98	7.74	18.2	161.05	3F	0.026	1.29	< 0.05	4.73	34.39	94.6	23.73	56.16	PV03	**0.073**	0.032
												8F	0.024	1.21									

proportion of clay minerals and Fe oxides (DD1705 and DD1706). As a result of the dissolving of the limestones, the pH and EC values increased during the test (Table 2). These findings suggest that both dissolution and desorption processes can lead to As release.

Physicochemical characterization of water

The physicochemical characteristics of the sampled waters are listed in Table 1. The concentrations of As and F^- in the wells (PV03 and SJMer) exceeded those allowed by NOM-127-SSA1-1994- (modified 2000). The well temperatures were 39.52°C for PV03 and 45.69°C for SJMer. According to research conducted in the area, both wells display characteristics of a low-temperature geothermal system (Morales-Arredondo et al. 2018a, b, c Moran-Ramírez et al. 2020). The measured pH values were within the range of alkaline water, and redox measurements for both wells revealed oxidizing conditions. Hydrogen carbonate (HCO_3^-) and sodium (Na^+) ions were more prevalent than other ions in the concentrations of major elements (Fig. 4).

The Eh–pH diagrams indicate that the predominant As species in both wells was hydrogen arsenate ($HAsO_4^{2-}$; as As^V) (Fig. 4), which was confirmed by using selective cartridges for arsenate and measuring the concentration of arsenite in the laboratory using hydride generation atomic absorption spectrometry (Table 1). This information is crucial because the removal of As from water is controlled by the distribution and behavior of arsenic species, and the most effective arsenic remediation approach for drinking water removes arsenate (Webb and Davis 2016). The diagrams of the major species of fluoride in both wells revealed that F^- was the predominant ion (Fig. 4b, d).

Fluoride and arsenic removal experiments using synthetic solutions that simulate the groundwater content

Detailed below are the results of experiments using the three limestones to remove synthetic fluoride and arsenic solutions (with the NaF, and $Na_2HAsO_4{\cdot}7H_2O$ solutions) (Figs. 5 and 6 and Table 2).

The RC1701 sample, which had the highest $CaCO_3$ content, exhibited the most effective range of F^- removal efficiency (ranging from 43.88 to 47.86%) and the highest capacity for As removal (ranging from 94.71 to 95.39%) (Fig. 5a, b, Table 3), achieving a concentration of F^- below the NOM-127-SSA1 limit in the sample with an initial concentration of 2.8 mg/L. At 72 h, the final pH values for each sample ranged between 7.0 and 8.5, while the EC varied between 100 to 120 µS/cm.

The rock DD1706 achieved a high F^- removal efficiency ranging between 29.64 and 31.53%, while the highest As

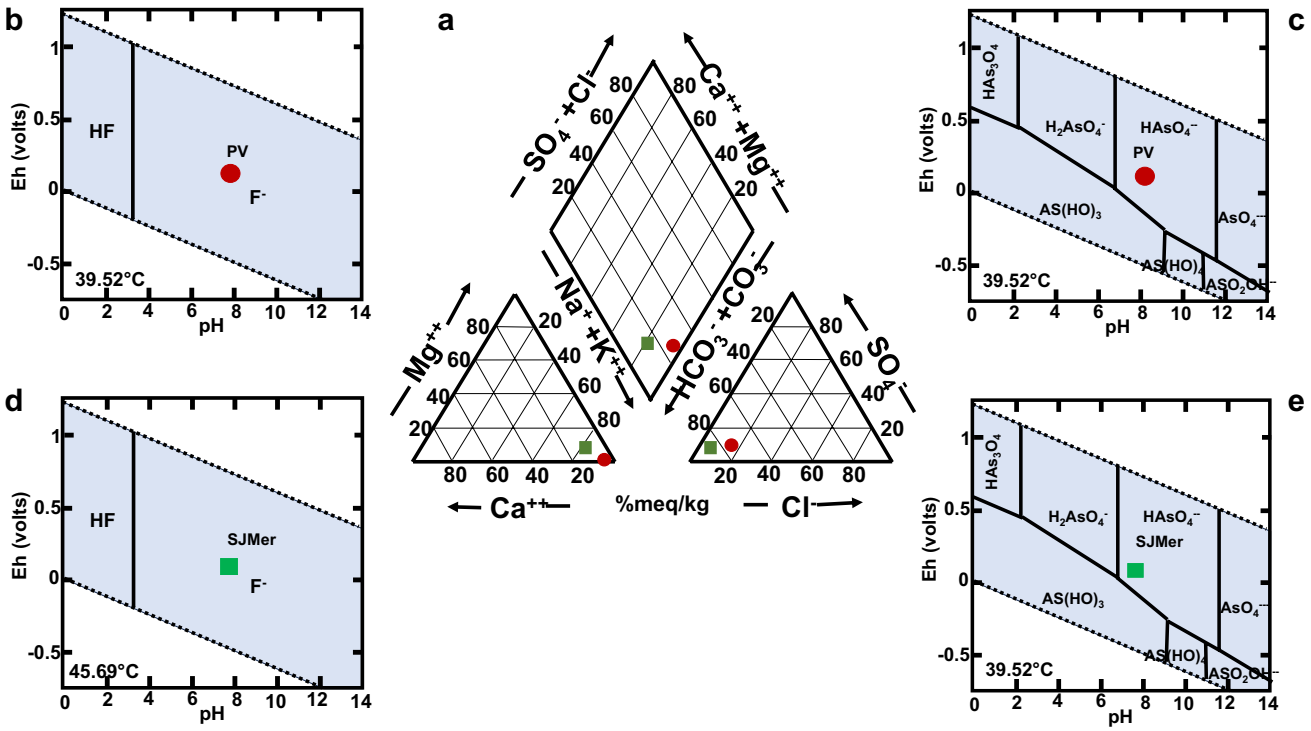

Fig. 4 **a** Piper diagram of PV03 and SJMer wells, **b** Eh–pH diagram of the aqueous species of F^- at 39.52° C for PV03 well, **c** Eh–pH diagram of the aqueous species of As at 39.52° C for PV03 well, **d** Eh–pH diagram of the aqueous species of $F.^-$ at 45.69° C for SJMer well, **e** Eh–pH diagram of the aqueous species of As at 45.69° C for SJMer well (Geochemist's Workbench program©)

removal was between 95.72% and 95.92% for both synthetic solutions, with a grain size < 0.05 mm (Fig. 5a, b; and Fig. 6a, b; Table 3), similar to DD1705 rock (SMF 2a and b, SMT 2 and 3). In contrast to other rocks of comparable grain size and smaller specific surface area, this rock demonstrated a relatively low F^- removal effectiveness (Fig. 5c, d; Fig. 6c, d; Table 3, SMF 2 and 3, SMT2 and 3).

In all experiments involving the three limestones and the synthetic solutions such as PV03 and SJMer water wells, the highest F^- removal efficiencies were obtained with a long time of rock–water interaction at the initial pH and the smallest grain size (< 0.05 mm) regardless of the specific surface area of the rocks. The rock with the highest $CaCO_3$ content and the smallest specific surface area resulted in the greatest % of removal (RC1701). In contrast, the rock DD1706 with the lowest $CaCO_3$ concentration and the greatest specific surface area showed the least efficacy..

In relation to the extraction of As from the three rocks, it was observed that the efficiency of removal exhibited a slight decrease as the duration of agitation increased for the grain size smaller than 0.05 mm. In contrast, an opposite trend was observed for the grain size ranging from 0.50 to 1.41 mm. Unlike F^-, which required a longer time for better elimination, the highest percentage of As removal was reached in the shortest time in an acidic solution (as the pH increased from ~ 5 to a range between 7.4 and 8.7).

Groundwater arsenic and fluoride removal tests

The water samples obtained from the PV03 and SJMer wells, in addition to the three limestone samples described below, were utilized for conducting batch tests..

The RC1701 had a greater capacity for removing As compared toF^- with the smallest grain size. Similarly, this rock removed up to 30.28% of F^- and 56.67% of As from the SJMer well water (Fig. 7; Table 3). The pH values observed ranged from 8.0 to 8.5, whereas the electrical conductivity values ranged from 400 to 550 µS/cm. This rock removed more As and F^- from SJMer well water when the grain size was < 0.05 mm (Fig. 8a, b; Table 3). Only four As removal experiments yielded concentrations lower than the NOM-127 maximum limit allowed for drinking water (0.025 mg/L). None of the F^- removal tests yielded concentrations below the maximum limit allowed by the drinking water standard (1.5 mg/L) with a F^- removal rate of 30.28% (Fig. 7a, b, Table 3; SMF 4; SMT3).

The highest percentage of As (52.08%) and F^- (23.94%) removal with the rock DD1706 was achieved with a grain size < 0.05 mm (Fig. 8a, b, Table 3), which was similar to DD1705 rock (SMF 5, SMT 2 and 3). The results indicated that the As and F^- removal effectiveness decreased with increasing agitation time (Figs. 7 and 8, Table 3); in particular, the removal process resulted in negative

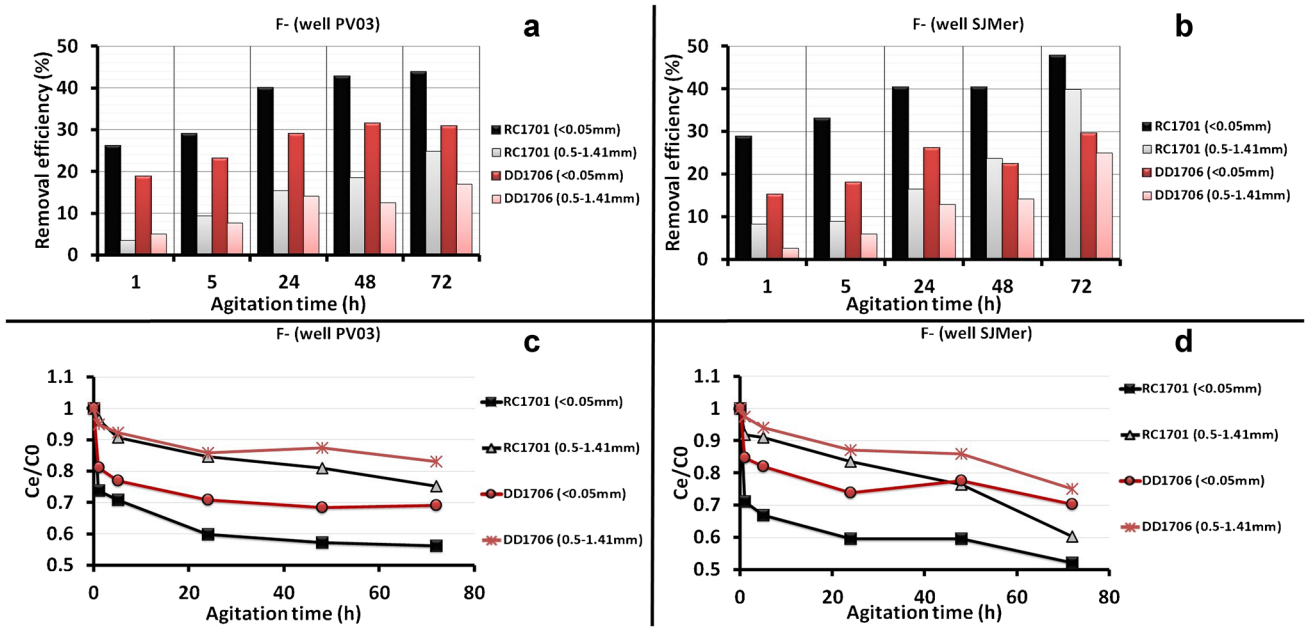

Fig. 5 Percentage of F^- removal using the concentration of each well. **a** Initial concentration of PV03 F^- = 7.2 mg/L with two grain sizes < 0.05 mm (black and red bars) and 0.5–1.41 mm (gray and pink bars) at agitation times of 1, 5, 24, 48, and 72 h, for rocks DD1706 and RC1701. **b** Initial concentration of SJMer F^- = 2.8 mg / L with two grain sizes < 0.05 mm (black and red bars) and 0.5–1.41 mm (gray and pink bars) at agitation times of 1, 5, 24, 48, and 72 h for DD1706 rock. **c** Pseudo-equilibrium diagrams of F^- concentration in the removal tests with rocks RC1701 and DD1706 for PV well. **d** Pseudo-equilibrium diagrams of F^- concentration in the removal tests with rocks DD1706 and RC1701 for SJMer well. C_0 and C_e correspond to the initial and equilibrium concentrations respectively

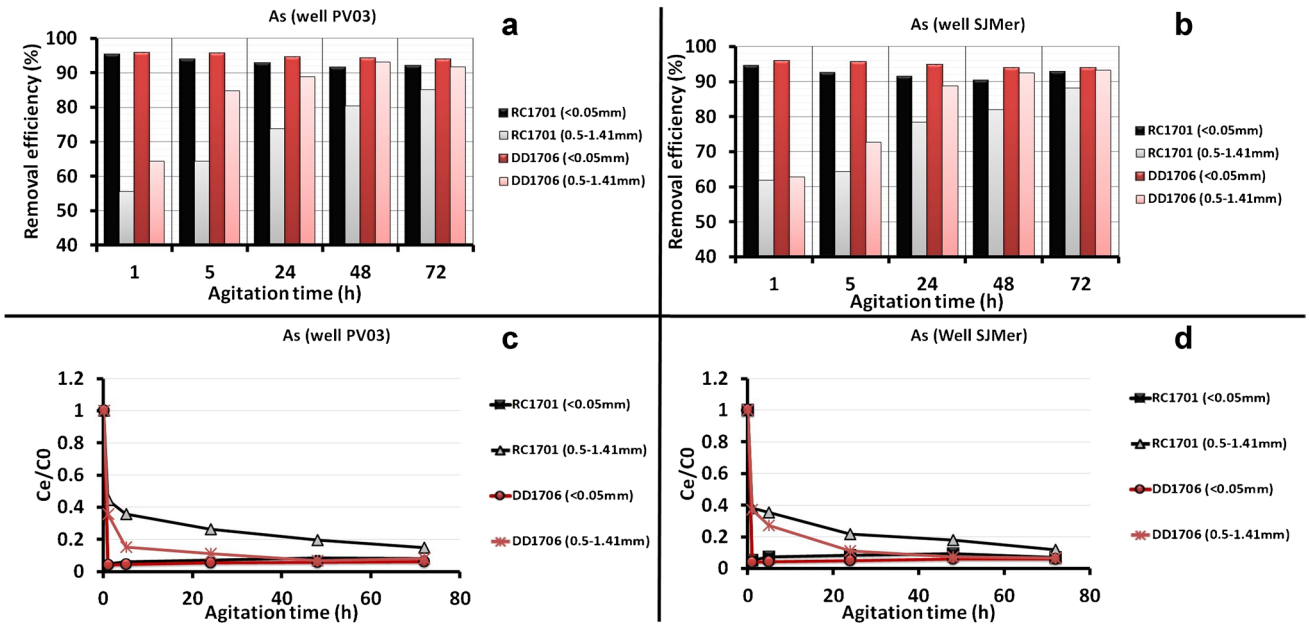

Fig. 6 Percentage of As removal with time in batch experiments with each rock. **a** PV03 concentration = 0.073 mg/L, two grain sizes < 0.05 mm (black and red bars) and 0.5–1.41 mm (gray and pink bars) of rocks DD1706 and RC1701 at stirring times of 1, 5, 24, 48, and 72 h. **b** SJMer concentration = 0.039 mg/L, two grain sizes < 0.05 mm (black and red bars) and 0.5–1.41 mm (gray and pink bars) of DD1706 rock. **c** Pseudo-equilibrium diagrams of As (initial concentration of PV03 well) experiments with DD1706 and RC1701 rocks. C_0 and C_e correspond to the initial and equilibrium concentrations respectively. **d** Pseudo-equilibrium diagrams of As (initial concentration of SJ Mer well), experiments with RC1701 and DD1706 rocks

Table 3 Removal efficiency corresponding to the studied rocks, grain size, synthetic solutions, and groundwater samples

Water type	Sample rock used	Grain size (mm)	Initial concentrations of the synthetic solution (mg/L)	The highest removal efficiency (%)	Water type	Sample rock used	Grain size (mm)	Initial concentrations of the synthetic solution (mg/L)	The highest removal efficiency (%)
synthetic solutions of fluoride	RC1701	<0.05	7.2	43.88	high fluoride contents in groundwater	RC1701	<0.05	7.2	25.79
	RC1701	<0.05	2.8	47.86		RC1701	<0.05	2.8	30.28
	RC1701	0.50–1.41	7.2	24.76		RC1701	0.50–1.41	7.2	15.23
	RC1701	0.50–1.41	2.8	39.79		RC1701	0.50–1.41	2.8	19.01
	DD1706	<0.05	7.2	31.53		DD1706	<0.05	7.2	19.75
	DD1706	<0.05	2.8	29.64		DD1706	<0.05	2.8	23.94
	DD1706	0.50–1.41	7.2	16.92		DD1706	0.50–1.41	7.2	10.43
	DD1706	0.50–1.41	2.8	24.91		DD1706	0.50–1.41	2.8	8.45
synthetic solutions of arsenic	RC1701	<0.05	7.2	95.39	high arsenic contents in groundwater	RC1701	<0.05	7.2	50.27
	RC1701	<0.05	2.8	94.71		RC1701	<0.05	2.8	56.67
	RC1701	0.50–1.41	7.2	85.16		RC1701	0.50–1.41	7.2	35.62
	RC1701	0.50–1.41	2.8	88.17		RC1701	0.50–1.41	2.8	41.67
	DD1706	<0.05	7.2	95.79		DD1706	<0.05	7.2	46.58
	DD1706	<0.05	2.8	95.92		DD1706	<0.05	2.8	52.08
	DD1706	0.50–1.41	7.2	93.08		DD1706	0.50–1.41	7.2	19.18
	DD1706	0.50–1.41	2.8	95.92		DD1706	0.50–1.41	2.8	25

values for both wells, suggesting the release of As and F^- from the rock. In this rock, muscovite is found in low amounts (including the rock DD1705); this mineral could be responsible for the release of F^- at an alkaline (Agrawal et al. 1997) pH, as F^- is abundant in the structure of muscovite (Labastida et al. 2017; Yan et al. 2011; Zhao et al. 2008). At the end of the tests, the pH reached slightly alkaline levels and hardness increased. As content in SJMer well water was below the NOM-127 for safe consumption (Fig. 8c, d, Table 3).

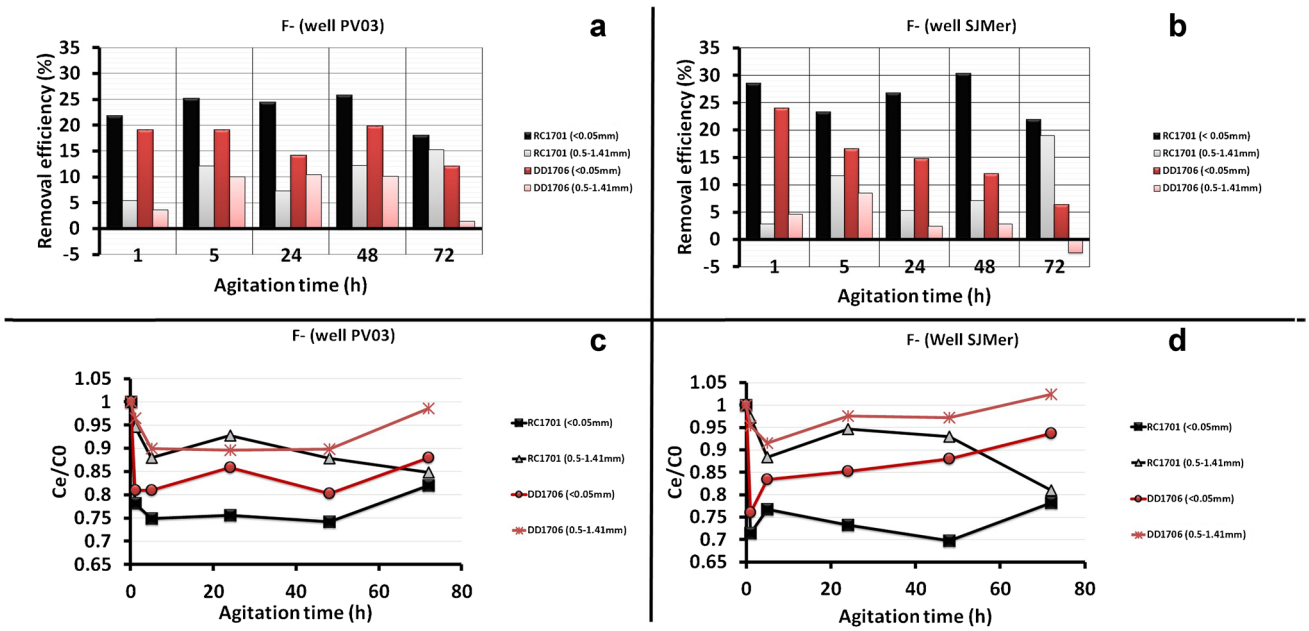

Fig. 7 Removal efficiency with time for **a** F^- in the water of PV03 well during the five agitation times with rocks RC1701 (black and gray bars), and DD1706 (red and pink bars), and **b** F^- in the water of SJMer well during the five stirring times for rocks RC1701 (black and gray bars), and DD1706 (red and pink bars), with two grain sizes (<0.05 and 0.5–1.41 mm). **c** Removal ratio (C_e/C_0) of F^- in PV well water for rocks RC1701 (black and gray bars), and DD1706 (red and pink bars), with two grain sizes (<0.05 and 0.5–1.41 mm). **d** Removal ratio (C_e/C_0) of F^- in SJMer well water for rocks RC1701 (black and gray bars), and DD1706 (red and pink bars), with two grain sizes (<0.05 and 0.5–1.41 mm). C_e = Equilibrium concentration, C_0 = Initial concentration

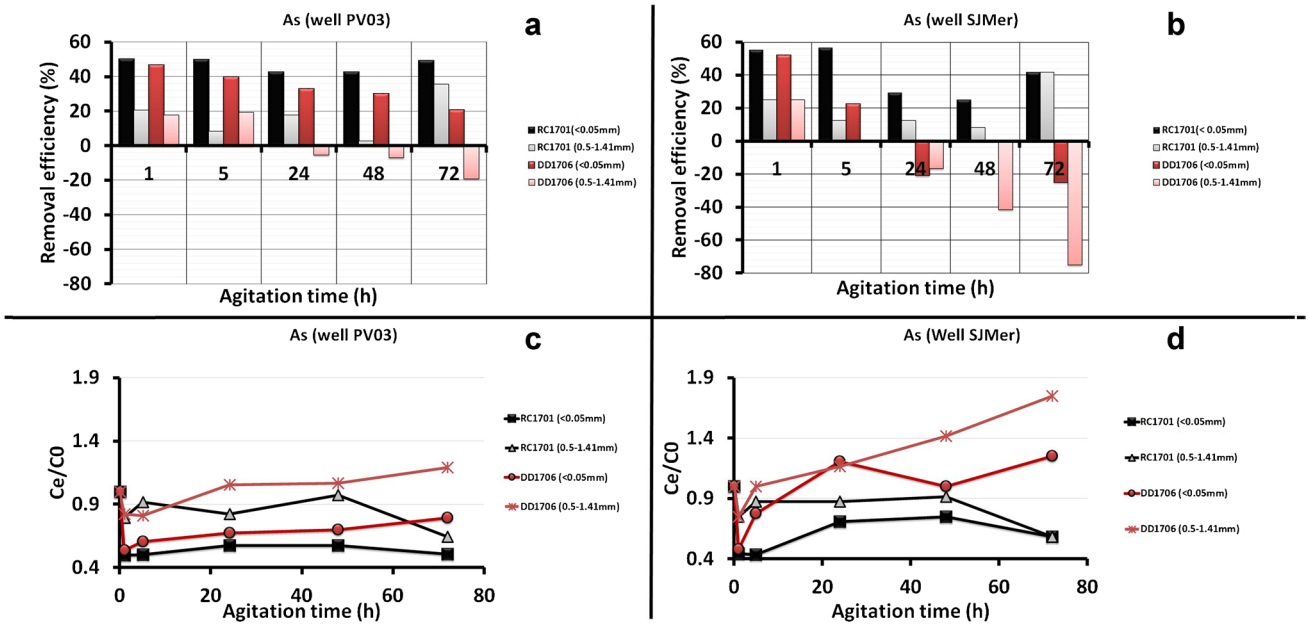

Fig. 8 Removal efficiency with time for **a** As in the water of PV03 well during the five agitation times for rocks RC1701 (black and gray bars), and DD1706 (red and pink bars). **b** As in the water of SJMer well during the five agitation times for rocks RC1701 (black and gray bars), and DD1706 (red and pink bars), with two grain sizes (<0.05 and 0.5–1.41 mm). **c** Removal ratio (C_e/C_0) of As in PV well water for rocks RC1701 (black and gray bars), and DD1706 (red and pink bars), with two grain sizes (<0.05 and 0.5–1.41 mm). **d** Removal ratio (C_e/C_0) of As in SJMer well water for rocks RC1701 (black and gray bars), and DD1706 (red and pink bars), with two grain sizes (<0.05 and 0.5–1.41 mm). C_e = Equilibrium concentration, C_0 = Initial concentration

Study of geochemical processes

The retention mechanisms of As and F^- in rocks were studied using semi-quantitative analysis by MEB-EDS before and after the removal experiments (the precipitates were analyzed in the rocks with a high removal percentage). The findings of the MEB-EDS analysis revealed a somewhat uniform distribution of As in the raw rocks. Although As was not detected in the semi-quantitative analysis, it was present in the samples and at sites with higher concentrations (Fig. 9a, b) after the tests than before (Fig. 9c, d). The EDS approach proved incapable of detecting the development of a mineral or complex species in the presence of F^- or As. However, despite the low concentration of As, its presence and distribution in the rocks after the batch tests indicates that the removal process does not produce a stable solid phase.

Hydrogeochemical modeling

To gain insight into the possible mechanisms involved in As and F^- removal, the saturation indices were calculated with GWB to identify the mineral phases that may be involved in the process. In the F^- removal tests (synthetic solution with NaF), calcite (SI = 0.011) and fluorite (SI = 0.200) were oversaturated, whereas in the As removal tests (synthetic solution with $Na_2HAsO_4{\cdot}7H_2O$), aragonite (SI = 0.350) and calcite (SI = 0.494) were oversaturated. Oversaturaion was not calculated for any As mineral. Positive saturation indices were found for chalcedony (SI = 0.968), cristobalite (SI = 0.768), and quartz (SI = 1.418) using water from the SJMer well. The saturation index results suggested that both calcite (SI = − 1.100) and fluorite (SI = − 0.737) might be involved in the dissolving process, as seen by the rise in Ca concentration during the experiments.

Fluorite (SI = 0.038), chalcedony (IS = 1.227), cristobalite (IS = 1.027), quartz (IS = 1.677), and sepiolite (IS = 1.183) were oversaturated based on the chemical parameters of the water in the PV03 well.

Notably, when comparing the two wells, PV03 contained the highest concentration of F^- (7.2mg/L), making fluorite formation more probable due to an increase in Ca^{2+} content from calcite dissolution, as demonstrated by prior research, and the positive fluorite SI (Reardon and Wang 2000; Labastida et al 2017). Using data from the SJMer well (lower F^- and As concentration), possible precipitation of fluorite was not identified; therefore, sorption may be the main removal process during all batch tests, as observed in other studies where external sphere complex processes control the content of F^- (Turner et al. 2005, Gogoi et al. 2015, Labastida et al. 2017).

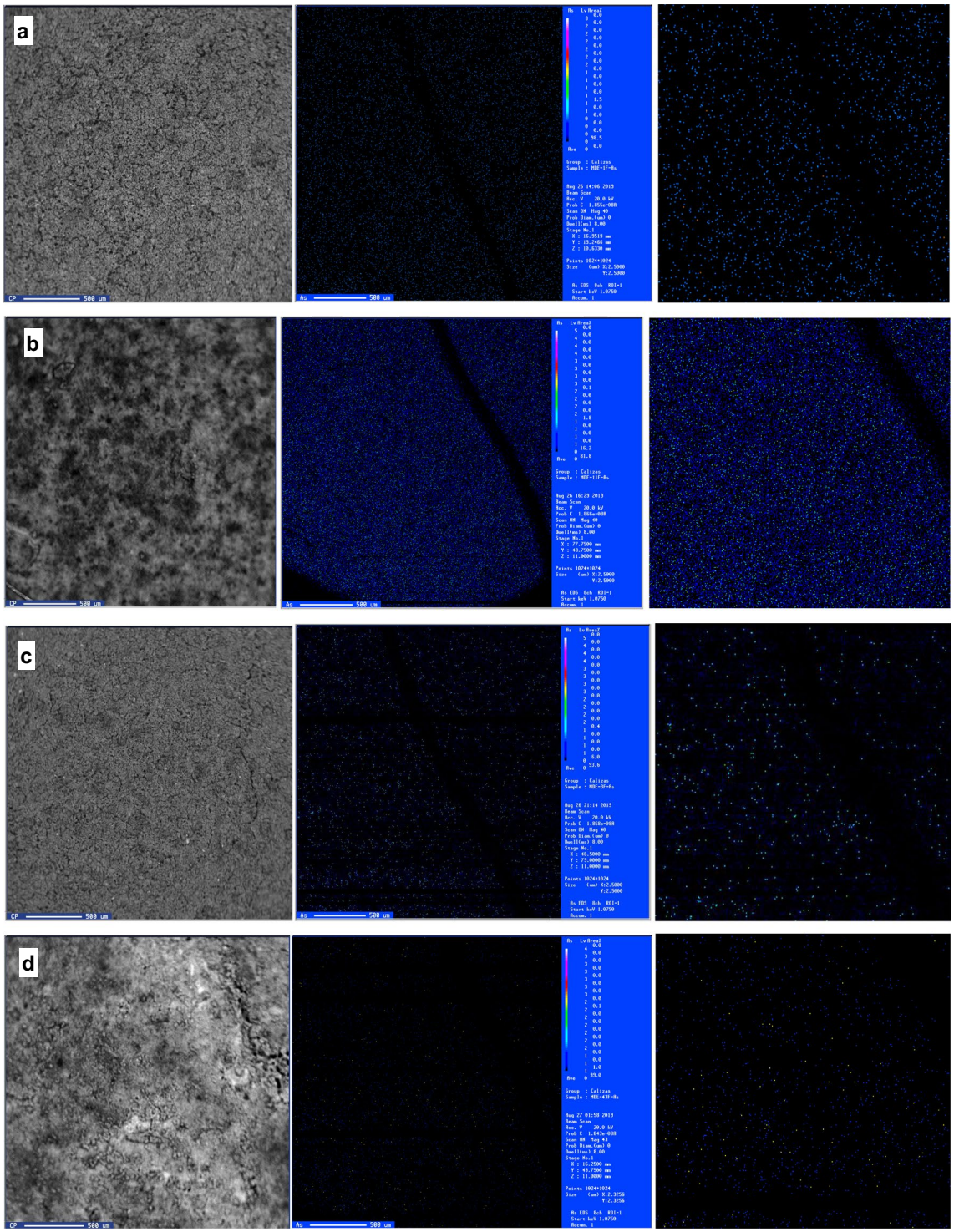

Fig. 9 **a** Image (left) and mapping of As (center) in rock RC1701 before treatment, **b** image and mapping of As in rock RC1701 after batch tests, **c** image and mapping of As in rock DD1706 before treatment, **d** image and mapping of As in rock DD1706 after batch tests

To better support the findings regarding the removal processes, Eh–pH diagrams were drawn for the solutions obtained after the three removal tests. The primary components contained in the water and released by the RC1701 rock were included.

The SI calculations matched the speciation depicted in SMF 6 where fluorite was the predominant mineral in water with a pH greater than 3.2 and when the Eh conditions were not as oxidizing (0.2–0.4 V). The F^- removal

experiments began at a pH range of 5.0–6.0 and ended at a pH range of 7.0 to 8.5. In addition, the EC values increased, which is consistent with the occurrence of fluorite precipitate caused by the dissolution of calcite and the high concentrations of F^- in the solution. The Eh values of the samples were not measured (the range of 0.2–0.4 V was used as the laboratory reference, standard conditions), so the diagrams are merely an approximation of the likely removal processes as observed in previous studies (Gogoi et al. 2015, Labastida et al. 2017).

SMF 6 reveals that the removal tests for As began with a pH range of 4 to 6, with the initial pH range and an Eh between 0.02 and 0.40; the precipitation of Ca $(AsO_2)_2$ would be favored up to a pH of 9. After this point, the dominant aqueous species was $CaAsO_4^-{}_{(a)}$ according to the Eh–pH diagram, and also observed in similar batch tests (Labastida et al. 2017).

Discussion

According to the results, it is likely that sorption processes of As and F^- are occurring simultaneously in the limestone or that sorption sites become occupied and there is no significant removal. This behavior has been reported in other studies; particularly when alkalinity increases, As removal decreases, and vice versa, this can be attributed to competition for sorption sites between arsenate and hydrogen carbonate (Van der Weijden et al. 1997). In additional experiments with calcium-hydrogen carbonate water and limestone rocks containing up to 89% $CaCO_3$, the greatest removal of more than 80% for As and more than 40% for F^- was reached; this removal was attributed to the Ca in the water, due to $CaCO_3$ dissolution (Manzo 2019).

Several studies have demonstrated that the immobilization of As, particularly As(V), can be effectively and rapidly achieved through sorption processes facilitated by calcite. The sorption behavior is also affected by pH because of changes in arsenate speciation or protonation/deprotonation of the sorbing arsenate (Román-Ross et al 2006), when pH increases (between 7 and 8) and due to the pHzpc of calcite (Romero et al. 2004) or forming a low-solubility precipitate of hydrated calcium arsenate ($Ca_5(AsO_4)_3OH$, known as arsenate apatite) (Webb and Davis 2016). Moreover, since arsenate desorption from calcite is rapid and complete within hours (Micete 2005, Sø et al. 2008), this process may be occurring in this test. The processes that govern the experimentally behavior observed are associated with sorption, which immobilizes As(V). However, a fraction of the immobilized As(V) is released within a few hours for both rock sizes (< 0.05 and 0.50–1.41 mm) because it is not integrated into the calcite.

As observed by Romero et al. (2004) and Micete (2005), grain size < 0.05 mm is susceptible to precipitation when the pH increases, primarily with As(V), generating low solubility precipitates (Sø et al. 2008, Webb and Davis 2016; Labastida et al. 2017). Moreover, it is well accepted that the removal of As can be achieved by precipitating Fe oxides, as this rock contains this element (Table 2). As removal in all rocks must be primarily governed by sorption mechanisms, although some mineral species may precipitate when the pH increases. Additionally, ionic strength can influence sorption through electrostatic effects. According to previous study, the sorbing arsenate species are H_2AsO_4 and $CaHAsO_4O$ (Sø et al. 2008).

Fluoride is removed either (1) by precipitation due to the increase of Ca^{2+} activity in the water, which is caused by the addition of compounds like lime, resulting in the supersaturation of water with fluorite (CaF_2) or (2) by sorption, and ion exchange reactions. In some tests, the use of limestone to remove high F^- contents, through CaF_2 precipitation, requires a low pH, which is obtained by adding CO_2 to generate carbonic acid (Reardon and Wang 2000). This method can make it difficult to change the pH, and CO_2 incorporation may not be suitable for rural applications. In additional experiments, the sorption/desorption process involving the formation of external sphere complexes and the precipitation of fluorite enables the limestones to remove between 60 and 65% of F^- (Labastida et al. 2017). In the same study, it was found that the removal of F^- depends on the $CaCO_3$ concentration and is constrained by its solubility product (Turner et al. 2005). When comparing these results with those presented in this study (Fig. 5), in which a trend was observed over time, the differences between the synthetic solutions and real groundwater are evident, as only F^- and As anions were present in the formers with an acidic pH, whereas in the tests with well water, in addition to the higher pH, other chemical species may affect the removal behavior, so competition between ions may be occurring during sorption and tentatively during precipitation.

As with the other batch tests, it is evident that simultaneous As and F^- removal occurs by sorption on the limestone, that this process is favored at a lower pH, and that the presence of Fe can influence As removal because it can precipitate and form Fe oxides (Romero et al. 2004, Van der Weijden et al. 1997). For F^- removal, fluorite may be precipitated as a result of the increase in Ca^{2+} activity upon calcite dissolution (Gogoi et al. 2015, Reardon and Wang 2000).

The observed differences in removal behavior within this study can be mostly attributed to the concurrent sorption–desorption processes involving As and F^- in the limestone, or to the competition between arsenate and hydrogen carbonate for sorption sites (when alkalinity increases,

As removal decreases). An additional issue to consider is the rise in pH which impacts the sorption behavior (and protonation/deprotonation) of arsenic (Román-Ross et al 2006). In the case of F^- removal, precipitation may be one of the primary processes, due to the increase of Ca^{2+} activity causing the formation of fluorite, and sorption/desorption may also occur, which involves the formation of external sphere complexes in addition to fluorite precipitation (Labastida et al 2017), However, in our experiment, the low removal was due to the relatively low proportion of $CaCO_3$, as reported by Turner et al (2005).

Lastly, this sample contains kaolinite, smectite, and muscovite type clays, but in all the studies conducted to evaluate the removal capacity of As and F^-, acidic or slightly acidic conditions (between 3 and 6) are required for the water for their retention (Chakraborty et al 2007; Mohapatra et al 2007; Nabbou et al. 2019; Mudzielwana and Gitari 2021) so that the alkaline conditions and pH between 7 and 8 of the groundwater suggest that these minerals do not contribute to the removal.

Results obtained with the NaF solutions and both water wells showed a greater removal efficiency at an acidic pH, where protons are retained on the surface of the functional groups, thereby increasing the positive charge (Acevedo et al. 2004; Ramos 2019). A more acidic pH can result in a greater dissolution of calcite, which can influence in a increase in Ca^{2+} activity (Reardon and Wang 2000). Further investigation has demonstrated that fluorite precipitation can be favored in an environment with an alkaline pH (8–8.5; SMF 6c). Therefore, both precipitation and sorption processes may be present during the removal of F^- from water (Nath and Dutta 2010). At this point, it is necessary to consider that the kinetic solubility of CaF_2 can be influenced by conditions such as temperature, the catalysts present, pressure, amount of solute, and water properties (the rate at which dissolution occurs and saturation is reached) (Christoffersen et al 1988, Sar et al. 2020; Salhov et al. 2013).

According to prior studies, the pH (> 7) and the $HAsO_4^{2-}$ species of As in the water could contribute to the formation of calcium arsenate (Zhu et al. 2006); however, a high As concentration should be required for this to occur (Renard et al. 2015). Our results suggest that the precipitation of calcium arsenate is not significantly favored at a pH of 8.18 (the pH of the PV03 well), because the pH is less than 9.0 and the concentration of arsenates in the water is low (SMF 6d). Another possible approach involves the co-precipitation of As onto calcite through the substitution of the carbonate group (Alexandratos et al. 2007). Overall, it is possible that the As removal from water by employing limestone rocks is the result of sorption–precipitation mechanisms. However, it must be considered that other significant factors influence the removal processes, as outlined as follows.

The removal percentages for each rock displayed fluctuation in the removal at various time intervals (Fig. 8), suggesting a diminished level of sorption during the As–rock as well as F^-–rock interactions. This phenomenon could potentially be associated to the formation of external sphere bonds as proposed by Zhan and Dixon (2004) and Labastida et al. (2017). The results additionally indicate that the presence of other anions in the well water may have resulted in competition forsorption sites, as is the case of sulfates and (bi) carbonates, which compete with arsenates and F^- (Sø et al. 2008; Sosa et al. 2020). In this work, the experiment was conducted with sodium–hydrogen carbonate water type contaning high HCO_3^- concentrations, which may displace the studied anions during sorption. The highest removal of As and F^- in well water experiments coincided with the lowest value of the calculated ionic strength (SJMer well), indicating that the sorption of these anions in the presence of hydrogen carbonate is more efficient at a lower ionic strength, as suggested by Sosa et al. (2020). Furthermore, while arsenates and fluoride have the ability to occupy surface sites (Zhu et al. 2007, and Bia et al. 2012), these anions do not exhibit competitive behavior with one another (Sosa et al. 2020).

The sorption of both As and F^- is dependent on the zero point of charge (ZPC) and specific surface area of the minerals present in rocks. The ZPC of calcite corresponds to a pH of 9.5 (Appelo and Postma 2004); consequently, calcite is the main mineral that contributes to the removal of the two contaminants, as observed in similar studies (Labastida et al. 2017), since both the pH of the well water and the synthetic solutions used in these studies were lower than the ZPC. This allowed for both the dissolution of calcite and the retention of anions. However, despite having low hematite concentrations, the pH corresponding to the ZPC ranges between 7.5 and 8.5 (Bowell 1994); this suggests that hematite might play a role in the adsorption of As. The effectiveness of DD1706 (and DD1705) in the removal of As in both experimental settings, namely the As solution and well water tests, is evident. Given that F^- was detected in the well water, it is feasible that muscovite played a significant role (by exerting a negative influence on the sorption process) in the well water experiments; it is necessary to mention that its ZPC is 7.5 (Labastida et al. 2017; Yan et al. 2011; Zhao et al. 2008). The sorption of the contaminating anion was not favored based on the observed pH of the well waters; therefore, muscovite does not contribute to the elimination of F^-, but rather to its concentration increase in the water through the release of F^-.

The results shown in Table 2 indicate that the specific area did not have a significant influence on the sorption of As or F^- by any of the rocks with the smallest grain size (< 0.05 mm) in the batch tests. The rock exhibiting the highest retention was the one with the lowest specific area (RC1701); however, the specific area only appears to

influence the retention for rocks with the largest grain size (0.50–1.41 mm), which explains why the smallest grain size produced better results (Table 2).

Calcite that has been exposed to water contains the functional groups $\equiv CO_3H$ and CaOH (Romero et al. 2004), which have a significant affinity for F^- and As. The removal of F^- is linked with calcite through different mechanisms, including the precipitation of fluorite during the dissolution of calcite, the ion exchange between F^- and CO_3^{2-}, and the surface sorption of F^- on calcite (Labastida et al. 2017; Sosa 2019). The removal of As may also be directly linked with calcite due to its dissolution, which can result in the precipitation of Ca arsenate (Labastida 2014; Romero et al. 2004; Sosa et al. 2020), the co-precipitation of As on calcite when the carbonate group is replaced, and the sorption of As on the surface of the calcite (Alexandratos et al. 2007; Romero et al. 2004; Sosa et al. 2020).

Due to the immense complexity of natural systems and retention processes, we were able to comprehend the processes that can occur when all of the chemistry found in drinking water is engaged due to the information collected utilizing well water. The next step would be to ascertain whether or not the laboratory pilot tests can be replicated at home. These experimental results could be supplemented by column experiments performed on the collected rocks in Guanajuato state as was performed in Soyatal rocks from Hidalgo state by Labastida et al. (2019) and Sosa et al. (2020).

Conclusions

According to the results, it can be observed that the amount of $CaCO_3$ and the grain size influences As and F^- removal. A high removal efficiency of As was achieved through the utilization of rocks containing a high $CaCO_3$ concentration. According to the modeling results, it was shown that the removal of F^- occurred by fluorite precipitation. However, sorption cannot be ruled out. When the pH increases, sorption processes can become the primary removal mechanism. Calcite shows a higher capacity for the elimination of arsenate in comparison to fluoride. The precipitation of calcium arsenate was not favored; however, we propose that the sorption–precipitation processes may operate in tandem to remove both As and F^- from the groundwater, but in a significantly greater proportion for As. The elimination of As and F^- from synthetic solutions was shown to be increased under conditions of acidic pH. The results of the synthetic solutions batch tests improved with increased agitation. The state of pseudo-equilibrium was attained after brief agitation times. According to sorption kinetic results, it would be more practicable to use a 1-h pseudo-equilibrium time when determining sorption isotherm, mainly for As (the maximum sorption efficiency of As). The limestones were more effective in removing As from synthetic solutions and well water than F^-. During the batch testing, it was observed that the RC1701 rock with a grain size < 0.05 mm removed the most As and F^-; with SJMer well water, this rock also did not release high amounts of As and F^- to the water despite having a greater initial As concentration compared to the other rocks. The removal percentages suggested that the retention of As and F^- was unstable, most likely due to sorption–desorption processes and to the formation of external sphere complexes, as corroborated by the ZPC value of calcite and the measured pH values. Furthermore, it is evident that in the well's water, competition occurs among anions primarily with sulfates and (bi) carbonates, which compete for sorption on active sites against arsenates and fluorides. Thus, there was not a significant removal of the ions of interest since the well water belonged to the sodium-hydrogen carbonate family, which has an alkaline pH and a high hydrogen carbonate concentration. Although MEB-EDS did not detect precipitation, the SI and the Eh–pH diagrams indicated the likelihood of fluorite formation (because this process is kinetically slow). The use of limestone rocks to remove As from well water yielded promising results, but those for F^- removal were less. The concentration of $CaCO_3$ should be the initial parameter to identify calcite rocks with the potential to be used to remove As and F^-.

For future evaluations, it is recommended that both major and trace elements (e.g., Ca^{2+}, Fe, Cd, Pb, P, and others) be taken into account. For instance, the trace elements can exert a substantial influence on the kinetics of calcite precipitation and dissolution, even though these processes frequently elude mathematical representation in the realm of geochemical modeling. An increase in the Ca^{2+} concentration in the drinking water (caused by the use of $CaCO_3$ in the elimination experiments) should also be checked, as a high Ca^{2+} concentration can be related to cardiovascular and kidney issues, and obstruct the absorption of other minerals if consumed by the general public.

Supplementary Information The online version contains supplementary material available at https://doi.org/10.1007/s12517-024-11896-6.

Acknowledgements The authors thank the support of O. Cruz and A. Aguayo from the "Laboratorio de Química Analítica" of the Institute of Geophysics, UNAM. We also thank R. Flores-Vargas and J.F. Landa-Arreguín for their help in the field campaigns.

Funding The study carried out in the region was financed by PAPIIT, grant numbers IN105023 and IN106918, and partial financial support was received from grant number IA101019.

DGAPA PAPIIT,IN105023,Fátima Juárez-Aparicio

Declarations

Ethical approval Not applicable.

Competing interests The authors declare no competing interests.

References

Acevedo O, Ortiz EH, Cruz MS, Cruz EC (2004) El papel de óxidos de hierro en suelos. Terra Latinoamericana 22(4):485–497. Retrieved February 15, 2024, from https://www.redalyc.org/pdf/573/57311096013.pdf

Agrawal V, Vaish AK, Vaish P (1997) Groundwater quality: focus on fluoride and fluorosis in Rajasthan. Curr Sci 73(9):743–746. Retrieved February 15, 2024, from https://www.jstor.org/stable/24100412

Alexandratos VG, Elzinga EJ, Reeder RJ (2007) Arsenate uptake by calcite: macroscopic and spectroscopic characterization of adsorption and incorporation mechanisms. Geochim Cosmochim Acta 71(17):4172–4187. https://doi.org/10.1016/j.gca.2007.06.055

APHA (2005) Standard methods for the examination of water and wastewater 21st edition American public health association, Washington DC. Retrieved October 22, 2023, from https://www.worldcat.org/title/standard-methods-for-the-examination-of-water-and-wastewater/oclc/156744115

Appelo CA, Postma D (2004) Geochemistry, groundwater and pollution, 2nd edn. A.A. BALKEMA PUBLISHERS, Great Britain

Armienta MA, Segovia N (2008) Arsenic and fluoride in the groundwater of Mexico. Environ Geochem Health 30:345–353. https://doi.org/10.1007/s10653-008-9167-8

Armienta MA, Rodríguez R, Aguayo A, Ceniceros N, Villaseñor G, Cruz O (1997) Arsenic contamination of groundwater at Zimapán México. Hidrogeol J 5(2):39–46

Baez LJA (2012) Estratigrafía de la parte sur del distrito minero de Guanajuato, México. Tesis de maestría, Universidad Nacional Autónoma de México, Centro de Geociencias, Querétaro, México. Retrieved February 15, 2024, from https://repositorio.unam.mx/contenidos/78087

Bia G, De Pauli CP, Borgnino L (2012) The role of Fe (III) modified montmorillonite on fluoride mobility: adsorption experiments and competition with phosphate. J Environ Manage 100:1–9. https://doi.org/10.1016/j.jenvman.2012.01.019

Bowell RJ (1994) Sorption of arsenic by iron oxides and oxyhydroxides in soils. Appl Geochem 9:279–286. https://doi.org/10.1016/0883-2927(94)90038-8

Bundschuh J, Armienta MA, Morales-Simfors N, Ayaz-Alam M, López DL, Delgado-Quezada V, Dietrich S, Schneider J, Tapia J, Sracek O, Castillo E, Lue-Meru MP, Altamirano-Espinoza M, Guimarães-Guilherme LR, Nahuel-Sosa N, Khan-Niazi N, Tomaszewska B, Lizama-Allende K, Bieger K, Alonso DL, Brandão PFB, Bhattacharya P, Litter MI (2021) Arsenic in Latin America: new findings on source, mobilization and mobility in human environments in 20 countries based on decadal research 2010–2020. Crit Rev Environ Sci Technol 51(16):1727–1865. https://doi.org/10.1080/10643389.2020.1770527

Chakraborty S, Wolthers M, Chatterjee D, Charlet L (2007) Adsorption of arsenite and arsenate onto muscovite and biotite mica. J Colloid Interface Sci 309(2):392–401. https://doi.org/10.1016/j.jcis.2006.10.014

Christoffersen J, Christoffersen MR, Kibalczyc W, Perdok WG (1988) Kinetics of dissolution and growth of calcium fluoride and effects of phosphate. Acta Odontol Scand 46(6):325–336. https://doi.org/10.3109/00016358809004784

CONAGUA (Comisión Nacional del Agua) (2015) Actualización de la disponibilidad media anual de agua subterránea acuífero (1115) valle de Celaya, Estado de Guanajuato. Gerencia de evaluación y ordenamiento de acuíferos. Diario oficial de la Federación Recuperado de. Retrieved February 15, 2024, from https://www.gob.mx/cms/uploads/attachment/file/103024/DR_1115.pdf

Echegoyén SJ, Romero MS, Velázquez SS (1970) Geología y yacimientos minerales de la parte central del Distrito Minero de Guanajuato. Consejo de Recursos Naturales No Renovables Boletín 75 1 36

Edmunds WM, Smedley PL (2013) Fluoride in natural waters. En O. Selinus. (Ed.), Essentials of Medical Geology pp. 311–336 Alemania, Heildelberg: Springer. http://nora.nerc.ac.uk/id/eprint/20520/

Gogoi S, Kath SN, Bordoloi Sh, Dutta RK (2015) Fluoride removal from groundwater by limestone treatment in presence of phosphoric acid. J Environ Manage 152:132–139

Gonsebatt ME, Del Razo LM (2018) Efectos a la salud por la exposición al arsénico. In book: Hacia el Cumplimiento del Derecho del Agua: Arsénico y Fluoruro en agua: riesgos y perspectivas desde la sociedad civil y la academia en México pp 57–62 Ciudad de México, México

Jiménez CMI, Cárdenas GM, Barbier OL (2018a) Efectos a la salud por la exposición a fluoruro. In book: Hacia el Cumplimiento del Derecho del Agua: Arsénico y Fluoruro en agua: riesgos y perspectivas desde la sociedad civil y la academia en México pp. 63–67 Ciudad de México, México. http://bajotierra.com.mx/recorrido/images/Biblioteca/paradigmas.pdf

Jiménez CMI, Cárdenas GM, Deogracias OPM, Del Razo LM (2018b) Estudios realizados en México relacionados a la exposición de arsénico y fluoruro. In book: Hacia el Cumplimiento del Derecho del Agua: Arsénico y Fluoruro en agua: riesgos y perspectivas desde la sociedad civil y la academia en México. 68–74 Ciudad de México, México. http://bajotierra.com.mx/recorrido/images/Biblioteca/paradigmas.pdf

Kefeni KK, Msagati TAM, Mamba B (2017) Acid mine drainage: prevention, treatment options, and resource recovery: a review. J Clean Prod 151:475–493. https://doi.org/10.1016/j.jclepro.2017.03.082

Labastida I, Armienta MA, Beltrán M, Caballero G, Romero P, Rosales MA (2017) Limestone as a sustainable remediation option for water contaminated with fluoride. J Geochem Explor 183:206–213. https://doi.org/10.1016/j.gexplo.2016.12.001

Labastida I, Armienta MA, Lara René Briones R, González I, Romero F (2019) Kinetic approach for the appropriate selection of indigenous limestones for acid mine drainage treatment with passive systems. Sci Total Environ 67:404–417. https://doi.org/10.1016/j.scitotenv.2019.04.373

Labastida I (2014) Evaluación de un sistema basado en rocas calizas, para tratar el drenaje ácido de mina en el distrito minero de Zimapán, Hidalgo (Tesis de doctorado). Universidad Nacional Autónoma de México Ciudad de México, México 132.248.9.195/ptd2014/junio/0714690/Index.html

Litter MI, Alarcón-Herrera MT, Arenas MJ, Armienta MA, Avilés M, Cáceres RE, Cipriani HN, Cornejo L, Dias LE, Fernández Cirelli A, Farfán EM, Garrido S, Lorenzo L, Morgada ME, Olmos-Márquez MA, Pérez-Carrera A (2012) Small-scale and household

methods to remove arsenic from water for drinking purposes in Latin America. Sci Total Environ 429:107–122

Manzo GM (2019) Remoción de arsénico y fluoruro de aguas subterráneas naturalmente contaminadas en Zimapán, Hidalgo mediante rocas calizas. Tesis de licenciatura, Universidad Nacional Autónoma de México. Ciudad de México México. Retrieved February 15, 2024, from https://repositorio.unam.mx/contenidos/remocion-de-arsenico-y-fluoruro-de-aguas-subterraneas-naturalmente-contaminadas-en-zimapan-hidalgo-mediante-rocas-c-3492145?c=J9BX9q&d=false&q=*:*&i=3&v=1&t=search_1&as=0

Mejía ZF, Valenzuela GJL, Aguayo SS Meza FD (2009) Adsorción de arsénico en zeolita natural pretratada con óxidos de magnesio Revista internacional de contaminación ambiental 25 (4):217–227. http://www.scielo.org.mx/pdf/rica/v25n4/v25n4a2.pdf

Mengelle-López JJ, Canet C, Prol-Ledesma RM, González-Partida E, Camprubí A (2013) Secuencia vulcano-sedimentaria La Esperanza (Cretácico Inferior) al norte de Guanajuato, México: Importancia en la exploración de sulfuros masivos vulcanogénicos Boletín de la Sociedad Geológica Mexicana 65(3):511–525. http://www.scielo.org.mx/pdf/bsgm/v65n3/v65n3a6.pdf

Miaojun W, Jianhua W, Wenqu L, Qixiao Z, Fengmei S, Yuanhang W (2021) Groundwater geochemistry and its impacts on groundwater arsenic enrichment, variation and health risks in Yongning County, Yinchuan Plain of Northwest China. Exposure and Health. https://doi.org/10.1007/s12403-021-00391-y

Micete S (2005) Diseño de una planta piloto basada en adsorción en rocas calizas para el tratamiento del agua contaminada con arsénico del pozo Zimapán V en el Municipio de Zimapán, Hidalgo. (Tesis de maestría). Universidad Autónoma Metropolitana Ciudad de México, México

Mohapatra D, Mishra D, Chaudhury GR, Das RP (2007) Arsenic (V) adsorption mechanism using kaolinite, montmorillonite and illite from aqueous medium. Environ Sci Health A Tox Hazard Subst Environ Eng 42(4):493–499. https://doi.org/10.1080/10934520601187666

Morales JI, Rodríguez R, Armienta MA, Villanueva RE (2016a) A low-temperature geothermal system in central Mexico: hydrogeochemistry and potential heat source. Geochem J 50(3):211–225. https://doi.org/10.2343/geochemj.2.0406

Morales JI, Rodríguez R, Armienta MA, Villanueva RE (2016b) The origin of groundwater arsenic and fluorine in a volcanic sedimentary basin in central Mexico: a hydrochemistry hypothesis. Hydrogeol J 24(4):1029–1044. https://doi.org/10.1007/s10040-015-1357-8

Morales-Arredondo JI, Armienta MA, Rodríguez R (2018) Estimation of exposure to high fluoride contents in groundwater supply in some villages in Guanajuato. Mexico Tecnología y Ciencias del Agua 9(3):156–179. https://doi.org/10.24850/j-tyca-2018-03-07

Morales-Arredondo JI, Esteller MV, Armienta MA, Martínez TAK (2018b) Characterizing the hydrogeochemistry of two low temperature thermal systems in Central Mexico. J Geochem Explor 185:93–104. https://doi.org/10.1016/j.gexplo.2017.11.006

Morales-Arredondo JI, Armienta Hernández MA, Lugo-Dorantes AE, Barrera Arrazola AP, Flores-Ocampo IZ, Flores-Vargas R (2022) Fluoride presence in drinking water along the southeastern part of El Bajio Guanajuatense, Guanajuato, Mexico: sources and health effects. Environ Geochem Health 45(6):3715–3742. https://doi.org/10.1007/s10653-022-01426-2.F.I.=2.566(Q1)

Morales-Arredondo JI, Armienta Hernández MA, Hernández-Mendiola E, Estrada-Hernández RE, Morton-Bermea O (2018c) Hydrochemical behavior of uranium and thorium in rock and groundwater samples from southeastern of El Bajío Guanajuatense, Guanajuato, Mexico. Env Earth Sc 77:567. Retrieved February 15, 2024, from https://link.springer.com/article/10.1007%2Fs12665-018-7749-z

Moran-Ramírez J, Morales-Arredondo JI, Armienta Hernández MA, Ramos-Leal JA (2020) Quantification of the mixture of hydrothermal and fresh water in tectonic valleys. J Earth Sci. https://doi.org/10.1007/s12583-020-1294-x

Mudzielwana R, Gitari MW (2021) Removal of fluoride from groundwater using MnO2 bentonite-smectite rich clay soils composite. Groundw Sustain Dev 14:100623. https://doi.org/10.1016/j.gsd.2021.100623

Nabbou N, Belhachemi M, Boumelik M, Merzougui T, Lahcene D, HArek Y, Zorpas A A, Jeguirim M, (2019) Removal of fluoride from groundwater using natural clay (kaolinite): Optimization of adsorption conditions. C R Chim 22(2–3):105–112. https://doi.org/10.1016/j.jcis.2006.10.014

Nath SK, Dutta RK (2010) Fluoride removal from water using crushed limestone. Ind J Chem Technol 17:120–125. Retrieved February 15, 2024, from http://nopr.niscair.res.in/bitstream/123456789/7632/1/IJCT%2017%282%29%20120-125.pdf

WHO (World Health Organization) (2018) Fact sheets: arsenic. http://www.who.int/news-room/fact-sheets/detail/arsenic. Accesed 30 Nov 2018

Peiyue L, Xiaodong H, Yi L, Gang X (2019) Ocurrence and health implications of fluoride in groundwater of Loess Aquifer in the Chinese Loess Plateau: a case study of Tongchuan, Northwest China. Exposure and Health, 11:95–107. https://doi.org/10.1007/s12403-018-0278-x

Ramos ZQ (2019) Estudios de procesos de adsorción y retención competitiva de As, Pb y B, contenidos en aguas geotermales, en suelos agrícolas aledaños al campo geotérmico de Cerro Prieto Mexicali. Tesis de maestría, Universidad Nacional Autónoma de México, Ciudad de México. Retrieved February 15, 2024, from https://repositorio.unam.mx/contenidos/estudios-de-procesos-de-adsorcion-y-retencion-competitiva-de-as-pb-y-b-contenidos-en-aguas-geotermales-en-suelos-agrico-3479979

Reardon EJ, Wang Y (2000) A limestone reactor for fluoride removal from wastewaters. Environ Sci Technol 34(15):3247–3253. https://doi.org/10.1021/es990542k

Renard F, Putnis CV, Montes-Hernandez G, Ruiz-Agudo E, Hovelmann J, Sarret G (2015) Interactions of arsenic with calcite surfaces revealed by in situ nanoscale imaging. Geochim Cosmochim Acta 159:61–79. https://doi.org/10.1016/j.gca.2015.03.025

del Río-Varela P, Nieto-Samaniego AF, Alaniz-Álvarez SA, Ángeles-Moreno E, Escalona-Alcázar FJ, del Pilar-Martínez A (2020) Geología y estructura de las sierras de Guanajuato y Codornices, Mesa Central, México. Bol Soc Geol Mex 72 no.1. https://doi.org/10.18268/bsgm2020v72n1a071019

Rodríguez R, Morales I, Armienta A, Villanueva R, Segovia N (2015) Geothermal systems of low temperature in Mexican Highlands: alternative uses and associated risks. Procedia Environ Sci 25:214–219. https://doi.org/10.1016/j.proenv.2015.04.029

Rodríguez R, Armienta MA, Berlin J, Mejía JA (2001) Arsenic and lead pollution of the Salamanca aquifer, Mexico: origin, mobilization and restoration alternatives. Groundw Qual Nat Enhanced Rest Groundw Pollut (275):561–565. Retrieved February 15, 2024, from https://www.cabdirect.org/globalhealth/abstract/20023193830

Román-Ross G, Cuello GJ, Turrillas X, A, Fernandez-Martinez, L, Charlet, (2006) Arsenite sorption and co-precipitation with calcite. Chem Geol 233:328–336. https://doi.org/10.1016/j.chemgeo.2006.04.007

Romero F, Armienta MA, Carillo A (2004) Arsenic sorption by carbonate-rich aquifer material, a control on arsenic mobility at Zimapán, México. Arch Environ Contam Toxicol 47(1):1–13. https://doi.org/10.1007/s00244-004-3009-1

Salhov S, Aizenshtein M, Froumin N, Barzilai S, Frage N (2013) Dissolution kinetics and solubility limit of CaF_2 in molten

KCl–NaCl salt. J Mater Sci 48:3173–3176. https://doi.org/10.1007/s10853-012-7095-6

Sar S, Samuelsson C, Engström F, Ökvist LS (2020) Experimental study on the dissolution behavior of calcium fluoride. Metals 10(8):988. https://doi.org/10.3390/met10080988

Sdiri A, Higashi T (2013) Simultaneous removal of heavy metals from aqueous solution by natural limestones. Appl Water Sci 3:29–39. https://doi.org/10.1007/s13201-012-0054-1

Sdiri A, Higashi T, Jamoussi F, Bouaziz S (2012) Effects of impurities on the removal of heavy metals by natural limestones in aqueous systems. J Environ Manage 93(1):245–253. https://doi.org/10.1016/j.jenvman.2011.08.002

Singh S, Kushwaha BP, Nag SK, Mishra AK, Bhattacharya S, Gupta PK, Singh A (2011) In vitro methane emission from Indian dry roughages in relation to chemical composition. Curr Sci 101(1):57–65

Sø HU, Postma D, Jakobsen R, Larsen F (2008) Sorption and desorption of arsenate and arsenite on calcite. Geochim Cosmochim Acta 72(24):5871–5884. https://doi.org/10.1016/j.gca.2008.09.023

Sosa A, Armienta MA, Aguayo A, Cruz O (2020) Evaluation of the influence of main groundwater ions on arsenic removal by limestones through column experiments. Sci Total Environ 727:138459. https://doi.org/10.1016/j.scitotenv.2020.138459

Sosa AS (2019) Aplicación de rocas calizas para la remediación de acuíferos contaminados. Tesis de maestría, Universidad Nacional Autónoma de México Ciudad de México México. Retrieved February 15, 2024, from https://ru.dgb.unam.mx/handle/DGB_UNAM/TES01000798981

Sparks DL (2005) Toxic metals in the environment: the role of surfaces. Elements 1(4):193–197. https://doi.org/10.2113/gselements.1.4.193

Turner BD, Binning P, Stipp SLS (2005) Fluoride removal by calcite: evidence for fluoride precipitation and surface adsorption. Environ Sci Technol 39:9561–9568. https://doi.org/10.1021/es0505090

Valverde J, Castillo F (2002) Inventario físico de los recursos minerales del municipio Santa Cruz de Juventino Rosas, Gto. Recuperado de. Retrieved February 15, 2024, from https://mapserver.sgm.gob.mx/InformesTecnicos/InventariosMinerosWeb/T1102VARJ0002_01.pdf

van der Weijden RD, Meima J, Comans RNJ (1997) Sorption and sorption reversibility of cadmium on calcite in the presence of phosphate and sulphate. Mar Chem 57:119–132. https://doi.org/10.1016/S0304-4203(97)00018-2

Webb CJ, Davis AD (2016) Remediation of arsenic in drinking water (chapter 3). In: States JC (ed) Arsenic: exposure sources, health risks, and mechanisms of toxicity. Wiley, Hoboken, pp 61–80

Xiaodong H, Peiyue L, Yujie J, Yuanhang W, Zhenmin S, Vetrimurugan E (2020) Groundwater arsenic and fluoride and associated arsenicosis and fluorosis in China: ocurrence, distribution and management. Expos Health 12:355–368. https://doi.org/10.1007/s10653-020-00520-7

Xiaodong H, Peiyue L, Jianhua W, Miaojun W, Xiaofei R, Dan W (2021) Poor groundwater quality and high potential health risks in the Datong Basin, northern Chine: research from published data. Environ Geochem Health 43:791–812. https://doi.org/10.1007/s12403-020-00347-8

Yan P, Lu M, Guan Y, Zhang W, Zhang Z (2011) Remediation of oil-based drill cuttings through a biosurfactant-based washing followed by a biodegradation treatment. Bioresour. Technol. 102:10252–10259. https://doi.org/10.1016/j.biortech.2011.08.074

Zhan CG, Dixon DA (2004) Hydration of the fluoride anion: structures and absolute hydration free energy from first-principles electronic structure calculations. J Phys Chem A 108(11):2020–2029. https://doi.org/10.1021/jp0311512

Zhao J, Gu J, Du J (2008) Climate and soil moisture environment during development of the fifth palaeosol in Guanzhong Plain. Sci China Ser D-Earth Sci 51:665–676. https://doi.org/10.1007/s11430-008-0047-y

Zhu YN, Zhang XH, Xie QL, Wang DQ, Cheng GW (2006) Solubility and stability of calcium arsenates at 25°C. Water Air Soil Pollut 169(1–4):221–238. https://doi.org/10.1007/s11270-006-2099-y

Zhu MX, Ding KY, Jiang X, Wang HH (2007) Investigation on co-sorption and desorption of fluoride and phosphate in a red soil of China. Water Air Soil Pollut 183(1–4):455–465. https://doi.org/10.1007/s11270-007-9394-0

Zhuang J, Yu GR (2002) Effects of surface coatings on electrochemical properties and contaminant sorption of clay minerals. Chemosphere 49(6):619–628. https://doi.org/10.1016/S0045-6535(02)00332-6